

MINISTRY OF SCIENCE AND HIGHER EDUCATION  
OF THE RUSSIAN FEDERATION  
Federal state autonomous educational institution of higher education  
“South Ural State University (National Research University)”  
Polytechnic institute  
Power engineering faculty  
Industrial Heat Power Engineering department  
Classifier number and the name of the Master's program  
13.04.01 “Heat Power Engineering and Heat Engineering”

THESIS WORK  
IS VERIFIED BY  
Director  
of Repair & constructions Ltd.  
\_\_\_\_\_ K.A. Khasanov  
« \_\_\_\_\_ » \_\_\_\_\_ 2020

ALLOW TO DEFEND  
Head of department  
“Industrial Heat Power Engineering”  
Candidate of technical sciences,  
associate professor  
\_\_\_\_\_ K.V. Osintsev  
« \_\_\_\_\_ » \_\_\_\_\_ 2020

**Research on the Thermal System Optimization of Carbon Capture in Solar  
Assisted Coal Fired Power Plant**

THESIS WORK OF THE MASTER'S PROGRAM  
“HEAT POWER ENGINEERING”  
SUSU-13.04.01.2020.286.YY.EN TW

Head of the Master's program,  
Candidate of technical sciences,  
associate professor  
\_\_\_\_\_ K.V. Osintsev  
« \_\_\_\_\_ » \_\_\_\_\_ 2020

Head of work,  
Professor, PhD  
\_\_\_\_\_ E.V. Solomin  
« \_\_\_\_\_ » \_\_\_\_\_ 2020

Author of work,  
Student of Master's program  
of P-284 group  
\_\_\_\_\_ K. Gao  
« \_\_\_\_\_ » \_\_\_\_\_ 2020

Chelyabinsk 2020

MINISTRY OF SCIENCE AND HIGHER EDUCATION  
 OF THE RUSSIAN FEDERATION  
 Federal state autonomous educational institution of higher education  
 “South Ural State University (National Research University)”  
 Polytechnic institute  
 Power engineering faculty  
 Industrial Heat Power Engineering department  
 Classifier number and the name of the Master's program  
 13.04.01 “Heat Power Engineering and Heat Engineering”

ALLOW TO DEFEND  
 Head of department  
 “Industrial Heat Power Engineering”  
 Candidate of technical sciences,  
 associate professor  
 \_\_\_\_\_ K.V. Osintsev  
 « \_\_\_\_\_ » \_\_\_\_\_ 2020

### ANNOTATION

Kaixuan.Gao. Research on the Thermal System Optimization of Carbon Capture in Solar Assisted Coal Fired Power Plant. – Chelyabinsk: SUSU, PI, PEF; 2020, 79 pages, 16 tables, 18 figures, 59 references.

1. Take the 1000MW coal-fired unit as the research object, use the EBSILON software to simulate the production and operation of the coal-fired power plant under the condition that the VWO valve is fully opened, and compare it with the performance parameters of the power plant during actual operation to verify the accuracy of the EBSILON software.

2. Analyze the characteristics of the monoethanolamine carbon capture system, calculate the energy consumption and various thermal performance parameters of the carbon capture system, simulate the coal-carbon capture simulation, and analyze the steam extraction from different steam sources As a result, the scheme with the least disturbance to the coal-fired unit and the best performance parameters is selected by comparing the thermodynamic performance indexes of different schemes.

					<i>13.04.01.2020.286.YY.EN TW</i>								
	<i>Page</i>	<i>Document #</i>	<i>Signature</i>	<i>Date</i>	<i>Research on the Thermal System Optimization of Carbon Capture in Solar Assisted Coal Fired Power Plant</i>								
<i>Student</i>	Gao kaixan									<i>Letter</i>	<i>Page</i>	<i>Pages</i>	
<i>Head of work</i>	Solomin									T	W	6	79
<i>N.controller</i>	Alabugina R.A									<i>SUSU</i>			
<i>Head of dep.</i>	Osintsev K.V.									<i>Department «Industrial Heat Power Engineering»</i>			

3. Analyze the type, parameters and performance of the trough solar collector, analyze the solar radiation intensity and influencing factors, take the optimal radiation intensity as the design radiation intensity, and integrate with the solar thermal utilization technology according to the carbon capture energy consumption characteristics, Different coupling methods are used to capture carbon dioxide in coal-fired power plants, and the thermodynamic performance and economic performance of each integrated system are analyzed and evaluated, and the optimal plan is selected.

4. Analyze the carbon capture system of solar-assisted coal-fired power station based on the second law of thermodynamics, find out the equipment with large loss and low efficiency, analyze the causes, and explore the equipment with greater energy saving potential At the same time, the efficiency evaluation of the different integration methods proposed.

					<i>13.04.01.2020.286.YY.EN TW</i>						
	<i>Page</i>	<i>Document #</i>	<i>Signature</i>	<i>Date</i>	<i>Research on the Thermal System Optimization of Carbon Capture in Solar Assisted Coal Fired Power Plant</i>						
<i>Student</i>	Gao kaixan								<i>Letter</i>	<i>Page</i>	<i>Pages</i>
<i>Head of work</i>	Solomin								<i>T</i>	<i>W</i>	<i>6</i>
									<i>SUSU</i>		
<i>N.controller</i>	<i>Alabugina R.A</i>								<i>Department «Industrial Heat Power Engineering»</i>		
<i>Head of dep.</i>	<i>Osintsev K.V.</i>										

# TABLE OF CONTENTS

ABSTRACT.....	9
1 INTRODUCTION.....	10
1.1 Research background.....	10
1.2 Research significance.....	11
1.3 Research status at home and abroad.....	11
1.3.1 Research status and development trend of solar-assisted coal-fired units.....	11
1.3.2 Research status and development trend of carbon capture and storage technology.....	13
1.3.3 Research on Integrated Technology of Carbon Capture in Solar-Assisted Coal-Fired Power Station.....	16
1.4 Research content of this paper.....	18
2 CHARACTERISTIC ANALYSIS OF CARBON CAPTURE SYSTEM.....	19
2.1 Introduction of carbon capture system based on monoethanolamine.....	19
2.1.1 The reaction mechanism.....	19
2.1.2 Process flow and material parameters.....	20
2.2 Energy consumption analysis of a carbon capture system.....	22
2.3 Thermal performance analysis of the system.....	24
2.3.1 Calculation of CO <sub>2</sub> emission rate from fixed combustion of coal.....	24
2.3.2 Unit circulating thermal efficiency.....	25
2.3.3 Standard coal consumption rate for power generation.....	27
2.3.4 Unit heat consumption rate.....	27
Chapter summary.....	28
3 STUDY ON CHARACTERISTICS OF SOLAR ENERGY SYSTEM.....	28
3.1 Trough solar collector.....	28

					<i>13.04.01.2020.286.YY EN</i>	<i>page</i>
<i>ИЗМ</i>	<i>Page</i>	<i>Document #</i>	<i>Signat.</i>	<i>Date</i>		7

3.2 The selection of radiation intensity.....	30
3.3 Evaluation model of solar-assisted coal-carbon capture system.....	33
3.3.1 Solar Photovoltaic Conversion Efficiency.....	33
3.3.2 Economic evaluation index.....	33
Chapter summary.....	36
4 MODELING AND SIMULATION OF COAL-FIRED UNIT CARBON CAPTURE SYSTEM.....	36
4.1 Modeling and validation of coal-fired units.....	37
4.2 Model establishment of carbon capture system for coal-fired units.....	39
4.2.1 Research on coupling scheme.....	39
4.2.2 Results analysis.....	44
Chapter summary.....	46
5 PERFORMANCE ANALYSIS OF THE CARBON CAPTURE SYSTEM FOR SOLAR ENERGY ASSISTED COAL-FIRED UNITS.....	47
5.1 Study on integrated system scheme.....	47
5.2 Thermal performance comparison.....	52
5.3 Exergy analysis.....	55
5.3.1 Exergic analysis model for each equipment.....	55
5.3.2 Exergic calculation results.....	60
5.4 Economic comparison.....	64
SUMMARY AND PROSPECT.....	69
REFERENCES.....	71

## ABSTRACT

Kaixuan.Gao. Research on the Thermal System Optimization of Carbon Capture in Solar Assisted Coal Fired Power Plant. – Chelyabinsk: SUSU, PI, PEF; 2020, 79 pages, 16 tables, 18 figures, 59 references.

Environmental and energy issues are currently important international issues that need to be resolved urgently. Coal combustion in China accounts for 76.8% of carbon dioxide emissions. Among them, the carbon emissions of thermal power generation account for about 38% of the country's total. Carbon capture technology is an effective measure to solve the large carbon emissions of thermal power generation and has broad development prospects. Solar energy, as one of the clean energy sources, is abundant in China and is the most ideal external clean energy source. Related national policies also indicate that the future development of the energy industry will focus on renewable clean energy sources.

This article takes a 1000MW coal-fired unit as a reference object, adds a carbon capture system, and captures the CO<sub>2</sub> emitted by the power plant. Due to the huge energy penalty caused by the addition of a carbon capture system, a solar-assisted coal-fired power plant carbon capture scheme is proposed. Solar thermal field replaces coal-fired power plants and carbon capture systems to do work to make up for energy losses. Six types of steam supply methods for carbon capture systems were proposed, and the proposed scheme was simulated and calculated using EBSILON thermal balance calculation software. The results were analyzed for thermodynamic performance. It was found that when the secondary reheat cooling section was used to supply steam, the unit cycle The thermal efficiency is the highest of the six extraction schemes, which is 44.06%. The CO<sub>2</sub> emission rate is the lowest, as low as 122.06g/(kWh). The standard coal consumption rate and heat consumption rate for power generation are the lowest. Based on the steam resupply scheme in the secondary reheating and cooling stage, three types of carbon capture schemes for solar-assisted coal-fired power plants were proposed. After calculation, the high-energy-consumption scheme for solar energy was used to make the CO<sub>2</sub> emission rate of coal-fired power plants Reduced 594.87g/(kWh), the decarbonization rate reached 85%. Based on the coal-carbon capture system, the output of the solar-assisted coal-carbon capture system has increased by 237.449MW, the cycle thermal efficiency has been increased by 9.59 percentage points, and the CO<sub>2</sub> emission rate has been reduced by 21.83g/(kWh). Economic indicators such as investment in coal saving, average solar carbon capture cost, and leveled power generation cost are introduced to analyze the integrated system. In order to analyze the

					<i>13.04.01.2020.286.YY EN</i>	<i>page</i>
						9
<i>ИЗМ</i>	<i>Page</i>	<i>Document #</i>	<i>Signat.</i>	<i>Date</i>		

energy distribution of the system and evaluate the rationality of the energy utilization of the system, this paper uses the unitary equilibrium analysis method to evaluate the integration method. The results show that the boiler damage is the largest among coal-fired units and coal-carbon capture units, accounting for more than 90% of the machine's damage, and the efficiency is the lowest.

## 1 INTRODUCTION

### 1.1 Research background

Since the end of the 20th century, climate change, especially global warming, has become more and more serious. Today's growing demand for energy is driven by rapid economic growth, with the apparent result of increased use of fuels, particularly conventional fossil fuels, which have become key energy sources since the industrial revolution. A large number of measured data show that the global average surface temperature is rising [1]. It is widely believed in the international community that the main cause of climate warming is the emission of a large number of greenhouse gases, among which CO<sub>2</sub> is one of the main components of greenhouse gases. According to the global atmospheric research emissions database, global CO<sub>2</sub> emissions reached 33.4 billion tons in 2011, up 48% from two decades ago. Emissions of carbon dioxide into the atmosphere have risen by more than 39 percent in the last century, from 280 parts per million before industrialisation, to a record high of 400 parts per million in May 2013. According to the forecast of the International Energy Agency (IEA) [2], the demand for fossil energy will still account for a large proportion in the next ten years, accounting for about 75%, and CO<sub>2</sub> emissions will reach 41.9 billion tons, The global average temperature will rise by 3.6 °C. If there is no policy to mitigate climate change, global GHG emissions in 2030 are expected to increase by 25% -90% compared with 2000, and the carbon dioxide equivalent concentration in the atmosphere will increase to 600-1550 ppm [3]. By 2050, greenhouse gas emissions must be reduced by 12% to control the global average temperature rise not to exceed 2 °C [4].

Solar energy, as one of the clean energy sources, is rich in production capacity resources in China. In more than 60% of China's total land area, the annual sunshine hours are more than 2000h, and the production capacity is equivalent to 1.7 trillion tons of coal. It is one of the most ideal external clean energy sources [5]. At present, solar thermal power generation technology is mainly used in small units of pure solar power generation and small steam turbine circulation systems. Due to the low efficiency of

					<i>13.04.01.2020.286.YY EN</i>	<i>page</i>
						10
<i>ИЗМ</i>	<i>Page</i>	<i>Document #</i>	<i>Signat.</i>	<i>Date</i>		

small turbines, the generating capacity of pure solar energy system is small, and solar energy resources are not fully utilized. Secondly, since solar radiation is constantly changing over time and energy output is intermittent, in order to solve this problem, solar thermal fields need to be equipped with heat storage devices, which makes the cost of power generation too expensive [6,7]. According to the distribution of solar energy radiation in China, most regions of China have abundant solar radiation resources, and the geographical location is suitable for the construction of thermal power generation industry, which provides favorable conditions for the generation of solar-assisted coal-fired power plants [8]. Coal-fired carbon capture system coupled with solar thermal field power generation, which can not only effectively utilize solar energy resources but also reduce carbon dioxide emissions, which is an effective way to realize energy conservation and emission reduction in China [9].

**1.2 Research significance**

The way to reduce greenhouse gas emissions is not only to increase the use of clean energy, but also to improve existing facilities with high carbon dioxide emissions through technological transformation. Carbon Capture and Storage (CCS) is an effective measure to reduce carbon emissions from thermal power generation [10]. According to the prediction of the International Energy Agency, the carbon dioxide emission reduction after the adoption of CCS technology will rise to 19% in the next 30 years, becoming the most contributing carbon emission reduction technology [11].

**1.3 Research status at home and abroad**

**1.3.1 Research status and development trend of solar-assisted coal-fired units**

The basic core of solar assisted generation (SAPG) technology is to use solar thermal energy to replace steam extraction from the renewable Rankine thermal cycle. In the traditional generator set, this part of steam extraction is used to preheat the feed water entering the boiler. Although the efficiency of the thermal cycle can be improved, the steam turbine's outlet power is also reduced due to reduced steam flow. Steam

					<i>13.04.01.2020.286.YY EN</i>	<i>page</i>
						11
<i>ИЗМ</i>	<i>Page</i>	<i>Document #</i>	<i>Signat.</i>	<i>Date</i>		



heating working medium, the replaced steam can continue to do work in the system, thereby improving the overall efficiency.

The research group of R.J.Zoschak and S.F.Wu[12] firstly proposed the complementarity between solar energy and coal-fired power stations. Through the analysis of the complementary system, it was concluded that more than 30% of solar energy would actually be lost due to the reduction of steam cycle efficiency, but the combination of solar energy and coal still has a certain cost advantage. The Eric Hu research group in Australia proposed that solar energy is coupled with the traditional fossil fuel power generation cycle. By using low-grade thermal energy instead of extracted steam to heat the feedwater in the renewable Rankine cycle, in the relatively low solar heating temperature range, traditional renewable The Rankine cycle can achieve relatively high efficiency and reduce greenhouse gas emissions [13]. Eric et al. [14] suggested that using the same fuel during peak hours, SAPG can help coal-fired power plants increase power generation by up to 5%, or maintain the same power generation capacity but reduce greenhouse gas emissions in the same range. The higher the heat source temperature, the more the system benefits. At different temperatures, different types of collectors can easily become heat carriers, increasing solar radiation energy to meet increased power requirements. A theoretical analysis was carried out using a coal-fired power plant in Victoria, Australia as an example [15]. New Delhi Ctr Energy Research Institute Reddy, V. Siva et al. [16] used optical analysis of linear Fresnel reflection (LFR) solar concentrators to predict the effect of focal length and reflector width on the local concentration ratio and tilt (  $\theta$  ) angle, The effects of liquid concentration ratio and inlet temperature on the LFR solar concentrator were analyzed by energy analysis and exergy analysis. The study found that by using solar collector-assisted feedwater heaters (SAFWH) to heat all low-pressure and high-pressure feedwater from coal-fired power plants with steam turbine extraction, an instantaneous increase in power generation capacity of approximately 20% was observed. By replacing the high-pressure feedwater heater with solar-assisted feedwater heating for steam reheating, coal consumption increased by 3.35%. Compared with a solar thermal power plant alone, the solar-assisted supercritical coal-fired thermal power plant has higher energy efficiency, and its efficiency is lower than that of a coal-fired supercritical thermal power plant. In addition, for solar-assisted water supply heating, the land area requirement is 4.78 hectares / MW.

Domestic study of using solar power and coal-fired units coupling first started in the North China Electric Power University, proposed by [17] Cui Yinghong solar energy coupled with coal-fired units mainly through the form of heat exchange, must follow the

					<i>13.04.01.2020.286.YY EN</i>	<i>page</i>
						12
<i>ИЗМ</i>	<i>Page</i>	<i>Document #</i>	<i>Signat.</i>	<i>Date</i>		

principle of "grade counterpart, cascade utilization", and the energy grade of coal-fired units span is very big, this is for two kinds of energy coupling provides a good condition. In 2009, Eric's research group and Yang yongping's research group concluded through simulation that solar energy assisted coal-fired power generation can effectively reduce the amount of coal burning, and the higher the level of solar energy replacing steam extraction, the higher the utilization efficiency of solar energy [17]. Subsequently, the coupling method of solar energy and coal-fired units was analyzed [18]. Taking the thermal economy of different heating units and different heating surfaces of the same capacity unit as an illustration, the solar energy conversion efficiency when coupled with different capacity units The rule is that high-power units > small-power units (assuming that the main steam flow is unchanged). Taking three typical areas as examples, several factors that affect the intensity of solar radiation are analyzed [19]. Hong Hui [20] of the Chinese Academy of Sciences used a 330MW power plant in Xinjiang, China as an example to analyze the impact of medium-temperature solar-assisted coal-fired power plants on coal-fired power plants under non-design conditions. Performance has certain advantages. In the same year, they also discussed the thermodynamic properties of solar-assisted coal-fired power plants with temperatures below 300 ° C [21], and found that the exergy loss of solar-assisted coal-fired power plants is lower than that of pure solar power. Comparing technical economy, the non-design performance and economic performance of solar-assisted coal-fired power plants are superior to solar power plants.

### **1.3.2 Research status and development trend of carbon capture and storage technology**

A. Compared with other industries, power plants have the characteristics of large, stable and concentrated carbon dioxide emissions [22], which can achieve large-scale carbon dioxide emission reduction. CCS is called "carbon capture and storage," which captures and sequesters CO<sub>2</sub> from the burning of coal in coal-fired power plants. At present, the common carbon capture technologies mainly include pre-combustion capture, oxy-fuel combustion and post-combustion capture [23]. This paper studies the capture of CO<sub>2</sub> from flue gas after coal combustion, that is, the carbon capture method after combustion [24].

B. Pre-combustion carbon capture is mainly applicable to IGCC (Integrated Gasification Combined Cycle) integrated gasification combined cycle power plant. The

					<i>13.04.01.2020.286.YY EN</i>	<i>page</i>
						13
<i>ИЗМ</i>	<i>Page</i>	<i>Document #</i>	<i>Signat.</i>	<i>Date</i>		

fossil fuel is mixed with air or oxygen and vaporized to produce a synthesis gas composed of CO and H<sub>2</sub>. Then, it is catalytically reacted with H<sub>2</sub> and H<sub>2</sub>O in a converter, where CO is converted to CO<sub>2</sub>, and more H<sub>2</sub> is produced at the same time. Through the physical adsorption reaction, CO<sub>2</sub> is separated out, and H<sub>2</sub> can be used as fuel for the combined cycle of power generation to generate electricity. Pre-combustion carbon capture has the characteristics of high concentration, small system, and low energy consumption, and has attracted widespread attention in many countries. In recent years, many large domestic power generation companies have begun to substantially promote the IGCC project.

C. Oxygen-rich combustion carbon capture, fuel combustion in an oxygen-rich environment, combustion oxygen from the combustion chamber after the removal of the relevant nitrogen atmosphere, the resulting flue gas mainly contains H<sub>2</sub>O and CO<sub>2</sub>. Oxygen-rich combustion and carbon capture require the addition of a cryogenic air separation unit (ASU) to generate oxygen for combustion, resulting in an increase in energy consumption, but with extremely high CO<sub>2</sub> concentration (>95%) [25]. Downstream, a compression and purification unit (CPU) is set to purify flue gas and remove nitrogen, argon, oxygen and other volatile components after condensation to achieve the required purity before compression and pipeline transportation. Due to the additional ASU and CPU units, the efficiency loss would be about 10 percentage points [26].

D. Carbon capture after combustion to capture carbon dioxide from treated flue gas and is widely used in the chemical processing industry. Post-combustion capture technology can be retrofitted to existing large-scale point sources in coal-fired power plants, cement manufacturing industries, or refineries, because these are the main sources of carbon dioxide emissions in the atmosphere. It mainly uses wet / dry adsorbents and adsorption / desorption principles to collect and capture carbon dioxide. In post-combustion capture technology, the exhaust gas is treated before combustion to reduce some particulate matter and various oxides in the flue gas [27]. The trap is usually located between the chimney and the flue gas desulfurization unit.

E. The research on carbon capture technology at home and abroad has achieved initial results. Leung et al. [28] analyzed various technologies and problems related to carbon dioxide capture, separation, transportation, storage and monitoring. They mentioned that the choice of specific carbon dioxide capture technology depends largely on the type of power plant and the fuel used. Post-combustion capture technology is generally considered to be the most suitable for coal-fired power plants due to its high efficiency and low cost. The route of carbon capture in China. Ledoux et al. [29] studied

					<i>13.04.01.2020.286.YY EN</i>	<i>page</i>
						14
<i>ИЗМ</i>	<i>Page</i>	<i>Document #</i>	<i>Signat.</i>	<i>Date</i>		

the capture of carbon dioxide in the flue gas of industrial incinerators on a laboratory scale. They proposed a method for evaluating the capture of carbon dioxide by the alkanolamine process in the flue gas of incinerators. A sustainable approach, formulating 30% by weight of monoethanolamine (MEA) in water as a reference solvent, determining data requirements, performing a consistent assessment of CO<sub>2</sub> capture in incinerator flue gas, and designing an innovative Pilot to conduct research. The degradation measurement device is completed by a multi-functional tool for large-scale study of process performance (energy cost and capture efficiency), process specifications and input gas composition to study the corrosion mechanism and corrosion control throughout the process loop. At present, the test device has been put into use, and the operation of the mixture of nitrogen and carbon dioxide is consistent with the previous data, thus verifying the data collection system, balance calculation and analysis methods.

F. The Shenhua CCS demonstration project in the Ordos Basin in China is the first and largest carbon dioxide full-chain brine aquifer storage project in Asia. The unique feature of the project is that carbon dioxide was injected into 18 sandstone formations at the same time, and the overlying coal seam was mined after the injection stopped in 2015. Li Xiaochun et al. [30] based on the background and geological conditions of the Shenhua CCS demonstration project. The coupling process of thermal-hydro-mechanical-chemical (THMC) in geological storage of carbon dioxide is introduced, and the key geomechanical issues are mapped to the THMC process accordingly. Many domestic universities and institutions have studied carbon dioxide capture technology through experiments and simulation experiments. Tsinghua University's Zeng Qing et al. Conducted experiments to study the absorption of CO<sub>2</sub> by the ammonia method. The results show that the ammonia method can capture carbon dioxide at a rate of more than 95%. The higher the ammonia concentration, the greater the carbon dioxide removal rate [31]. Zhu Dechen of Zhejiang University used semi-continuous experiments under normal pressure to mix amines with different properties to improve the overall performance of the absorbent. A comparative study was conducted on the regeneration characteristics of 29 mixed absorbents under the same experimental conditions, introducing enhancement factors and interactions. The coefficient is used to analyze the principle of mixing ratio of absorbents, and the selection of mixed absorbents is discussed in detail [32]. Dr. Rongrong Zhai of North China Electric Power University built a small bubbling fluidized bed experimental platform to study the changing rules of carbon dioxide concentration in the reactor and the factors affecting the absorption process, and to illustrate the coupling characteristics under different coupling modes by case analysis.

					<i>13.04.01.2020.286.YY EN</i>	<i>page</i>
						15
<i>ИЗМ</i>	<i>Page</i>	<i>Document #</i>	<i>Signat.</i>	<i>Date</i>		

### 1.3.3 Research on Integrated Technology of Carbon Capture in Solar-Assisted Coal-Fired Power Station

The energy penalty imposed on the original unit by the coupling of the carbon capture unit and the coal-fired power station is currently the biggest obstacle to applying CCS technology to power plants. To this end, scholars at home and abroad have proposed the idea of supplementing the coal-fired unit with external energy to supply energy to the coupling system to make up for energy losses. As a clean and renewable energy source, solar energy is the best external auxiliary energy source with large output, easy access, and no burden on the environment.

The concept of coupling solar energy with power plants for carbon dioxide capture originated from a patent. An international Wibberley patent in 2007 mentioned that the solar thermal energy is applied to the post-combustion carbon capture system to make up for the large amount of thermal energy consumed in the rich liquid desorber [36]. The research group of Professor Rochelle of the University of Texas in 2010 proposed a form of desorption instead of a desorption tower, which uses solar energy as a heat source [37]. Calcium cycle (CAL) is a promising post-combustion carbon dioxide capture and storage technology. Tregambi et al. [38] coupled CAL with a centralized solar (CSP) system so that all the heat energy required by the calciner is provided by renewable energy. They proposed a simple integrated CAL-CSP process solution that stores excess incident power during the day as a calcined sorbent and is used in the CAL circuit at night. Based on the population balance model of the adsorbent particles, the system's cyclic operation includes the parameters of the solar field and the main operating parameters (adsorbent residence time, adsorbent, CO<sub>2</sub> inlet molar ratio, fluidization rate, etc.) to the degree and efficiency of carbonation Analyzed. Japan's Pyong et al. [39] evaluated the carbon dioxide capture power generation system with solar energy and gasified coal as input energy. Two types of power generation systems are proposed and analyzed from the perspective of economic characteristics: a hybrid power generation system (system I) that captures carbon dioxide and a three-stage heat utilization power generation system (system II). In the evaluation, the conventional integrated gasification combined cycle power generation (IGCC) system was used as the reference system. They assumed that the proposed system was built in Albuquerque, USA and Osaka, Japan. Based on the higher calorific value, the net coal power efficiency of the proposed system I is estimated to be 51.0%, and the net power efficiency of the proposed system II is 40.1%. The efficiency of the conventional system drops to 32.7%. Taking the net coal power efficiency of the IGCC system without carbon dioxide capture as 43.7% as a reference, the proposed CO<sub>2</sub> emission

					<i>13.04.01.2020.286.YY EN</i>	<i>page</i>
						16
<i>ИЗМ</i>	<i>Page</i>	<i>Document #</i>	<i>Signat.</i>	<i>Date</i>		

reduction costs of Albuquerque systems I and II are 22100-23800 yen / ton and 21800-23000 yen / ton , Osaka is 37000-38700 yen / ton and 23300-24500 yen / ton. The results show that these costs are 43,800-48,400 yen / ton lower than the CO2 emission reduction costs of the IGCC system using CO2 capture.

Domestic research on carbon capture by solar-assisted coal-fired power plants has developed rapidly in the past two years. Tianjin University's Wang Fu [40] and others established a solar thermal chemical absorption auxiliary experiment system to study the system performance. They tested the parabolic trough and linear Fresnel reflective solar collectors and found that the operating parameter values can meet the requirements of the set parameters. The collector can provide the heat energy required by the reboiler, and its contribution depends mainly on For solar radiation. The solvent regeneration was studied by changing the input heat. The results show that the response time of the reboiler heat load is longer than that of the reboiler temperature and desorber pressure. Liu Liangxu et al. [41] estimated the potential of ammonia-based solar-assisted post-combustion carbon capture SPCC technology based on detailed solar radiation resource assessment (ie DNI, sunshine time) and solar collector STC performance. Compared with a parabolic trough collector (PTC), it is more attractive to use a vacuum tube (VT) as the STC for capturing carbon dioxide in an ammonia-based post-combustion carbon capture power plant. Chen Haipingren [42] of North China Electric Power University studied the coupling mechanism and system integration of solar energy collection system, CO2 emission reduction system and coal-fired power plant thermal system. Based on the equivalent heat drop method, the thermal economic changes of the new integrated system under different 100% THA, 75% THA, and 50% THA operating conditions are analyzed. The change trend of unit thermal economy under different carbon capture rates is obtained. If the capture rate increases, the relative degree of thermal economy will increase. On this basis, the integrated system has also been optimized to achieve low energy consumption and low cost carbon dioxide emissions. Zhai Rongrong et al. [43] studied a solar-assisted monoethanolamine-based carbon capture technology and a 1000MW coal-fired power plant integrated system (PG-CC). In the first system, the solar-assisted coal-fired power generation system adds MEA-based CO2 capture (SA-PG-CC), which uses solar thermal energy to heat the high-pressure feed water in the power plant, and the rich liquid desorption in the reboiler Energy is provided by low-pressure steam from coal-fired power generation systems. The second system integrates the power plant with a solar-assisted MEA-based CO2 capture system (SA-CC-PG) and uses solar energy to directly power the reboiler. Both systems were simulated in EBSILON Professional and Aspen Plus, and analyzed

					<i>13.04.01.2020.286.YY EN</i>	<i>page</i>
						17
<i>ИЗМ</i>	<i>Page</i>	<i>Document #</i>	<i>Signat.</i>	<i>Date</i>		

using thermoeconomic theory. The thermodynamic and economic performance of each system was evaluated based on power generation and carbon dioxide capture.

#### 1.4 Research content of this paper

According to the above research status at home and abroad, it can be seen that many CCS projects are in progress, and the research on carbon capture technology based on coal-fired power plants is becoming more and more perfect. The current research focus of scholars at home and abroad is how to reduce the disturbance and huge energy penalty caused by the addition of a carbon capture system to the original coal-fired unit. The coupling method of the carbon capture system and the coal-fired unit is particularly important. Solar energy-assisted coal-fired power plants for carbon capture are undoubtedly the best energy replenishment program. The difficulty is how to couple solar heat with coal-fired power generation and carbon capture systems. This article takes a domestic 1000MW coal-fired unit as an example, and adds a post-combustion carbon capture system. Through modeling and simulation of the coupled system, the optimal coupling scheme is found to make the carbon emission rate the lowest, the coal consumption rate the lowest, and the highest efficiency. Add solar auxiliary equipment on the basis of coal-carbon capture coupling system, and optimize the parameters of the integrated system in all aspects through system optimization.

The specific research contents are as follows:

1. Take the 1000MW coal-fired unit as the research object, use the EBSILON software to simulate the production and operation of the coal-fired power plant under the condition that the VWO valve is fully opened, and compare it with the performance parameters of the power plant during actual operation to verify the accuracy of the EBSILON software

2. Analyze the characteristics of the monoethanolamine carbon capture system, calculate the energy consumption and various thermal performance parameters of the carbon capture system, simulate the coal-carbon capture simulation, and analyze the steam extraction from different steam sources As a result, the scheme with the least disturbance to the coal-fired unit and the best performance parameters is selected by comparing the thermodynamic performance indexes of different schemes.

3. Analyze the type, parameters and performance of the trough solar collector, analyze the solar radiation intensity and influencing factors, take the optimal radiation intensity as the design radiation intensity, and integrate with the solar thermal utilization

					<i>13.04.01.2020.286.YY EN</i>	<i>page</i>
						18
<i>ИЗМ</i>	<i>Page</i>	<i>Document #</i>	<i>Signat.</i>	<i>Date</i>		

technology according to the carbon capture energy consumption characteristics, Different coupling methods are used to capture carbon dioxide in coal-fired power plants, and the thermodynamic performance and economic performance of the integrated system are analyzed and evaluated, and the optimal plan is selected. (4.1)

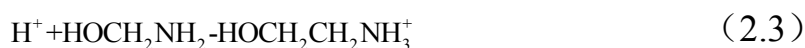
4. Analyze the carbon capture system of solar-assisted coal-fired power plant based on the second law of thermodynamics, find out the equipment with large loss and low efficiency, analyze the causes, and explore the equipment with greater energy saving potential. At the same time, the efficiency evaluation of the different integration methods proposed. (4.1)

## 2 CHARACTERISTIC ANALYSIS OF CARBON CAPTURE SYSTEM

### 2.1 Introduction of carbon capture system based on monoethanolamine

#### 2.1.1 The reaction mechanism

Alkanolamine represented by ethanolamine (MEA) is the main absorbent of the carbon capture technology of the alcoholamine method. Ethanolamine has a molecular formula of  $C_2H_5NH_2$  and is a strong alkaline hygroscopic liquid. It can rapidly react with carbon dioxide in the flue gas to form a more stable carbamate at a temperature of 20 to 50°C, thereby absorbing the CO<sub>2</sub>, this process is carried out in the absorption tower, the main chemical reaction formula is [45]:



Among them, reaction formula (2.4) is a reversible reaction. When the temperature is not high, the reaction proceeds from left to right, releasing heat; when the temperature

					<i>13.04.01.2020.286.YY EN</i>	<i>page</i>
						19
<i>ИЗМ</i>	<i>Page</i>	<i>Document #</i>	<i>Signat.</i>	<i>Date</i>		



is higher, the reaction proceeds from right to left, absorbing heat. The forward reaction occurs in the absorption tower, and the reverse reaction occurs in the desorption tower. When the temperature in the reboiler is higher than 105 °C, the carbamate undergoes a high-temperature endothermic reaction to release CO<sub>2</sub>, and at the same time, the ethanolamine liquid is decomposed to regenerate the MEA solution. The process of MEA rich liquid precipitation of CO<sub>2</sub> in the desorption tower requires a lot of energy consumption. This part of energy consumption can be provided by the steam extraction of the turbine at all levels, and it can also be directly provided by the solar energy system when coupled with the solar energy system.

### 2.1.2 Process flow and material parameters

The process flow of the carbon capture system is shown in Figure 2.1, Table 2.1 and Table 2.2 Main material parameters of the MEA carbon capture system [46]. The carbon capture system based on MEA solution mainly includes: absorption tower, desorption tower, reboiler, lean-rich liquid heat exchanger and other devices. As shown in Figure 2.1, the flue gas from the boiler is sent to the bottom of the absorption tower through dust removal, desulfurization, denitration and other equipment, and then flows from the bottom of the absorption tower to the top of the tower after being pressurized by the pressure booster. At the same time, the MEA lean liquid flows from the top of the tower to the bottom of the tower to chemically react with the treated flue gas in the absorption tower. The MEA lean liquid absorbs the CO<sub>2</sub> in the flue gas to generate MEA rich liquid. Discharge. Because the temperature of the chemical reaction in the desorption tower is higher than that of the absorption tower, the MEA rich liquid needs to absorb heat and heat up from the absorption tower before entering the desorption tower. The MEA rich liquid undergoes a chemical reaction in the desorption tower to decompose high concentration CO<sub>2</sub> and MEA lean solution. After CO<sub>2</sub> is cooled by the condenser, water vapor is removed and then stored. After condensation, the purity of CO<sub>2</sub> can reach 99.9%. The lean liquid with higher temperature will continue to cool after heat exchange through the rich-lean liquid heat exchanger. It will enter the absorption tower together with the MEA lean liquid supplemented into the carbon capture system to continue chemical reaction with a new cycle.

					<i>13.04.01.2020.286.YY EN</i>	<i>page</i>
						20
<i>ИЗМ</i>	<i>Page</i>	<i>Document #</i>	<i>Signat.</i>	<i>Date</i>		

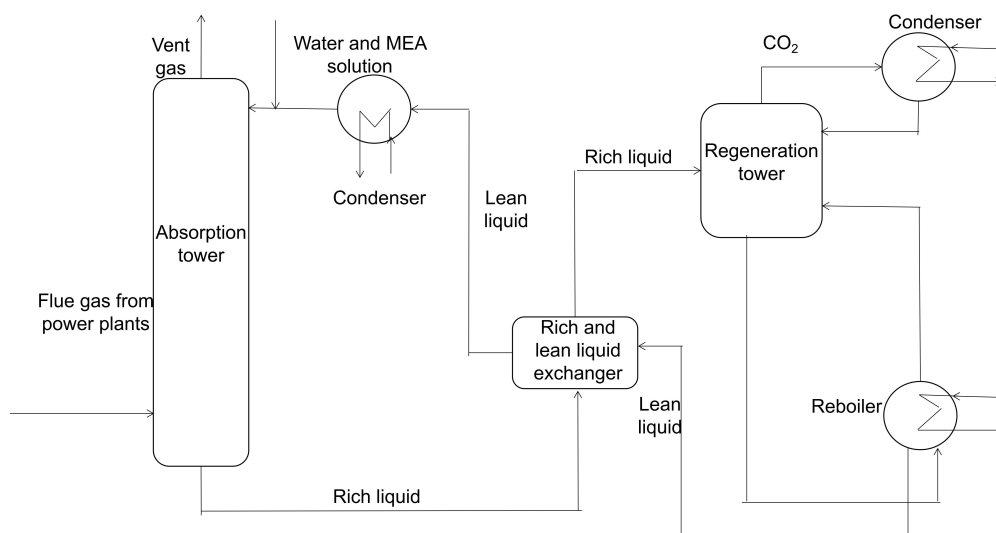


Figure 2.1 main process flow chart of MEA carbon capture system

Table 2.1 main material parameters of MEA carbon capture system -- gas [46]

Serial Number	Name	Pressure MPa	Temperature °C	Enthalpy MW	Specific heat kJ·kg·K-1	Composition%			
						CO <sub>2</sub>	N <sub>2</sub>	H <sub>2</sub> O	O <sub>2</sub>
1	Into the flue gas	0.108	40	30.088	3.71	14.45	75.0	7.13	3.30
2	Decarburization of flue gas	0.102	40	27.909	4.18	3.31	85.8	7.09	3.77
3	Overhead gas	0.150	98	71.978	12.13	35.54	0.17	64.3	0.00
4	Cooling tower	0.145	40	7.322	3.03	35.54	0.17	64.3	0.00
5	The product of CO <sub>2</sub>	0.145	40	3.025	2.13	94.93	0.46	4.61	0.00
6	Gaseous CO <sub>2</sub>	2.3	40	-	-	-	-	-	-
7	Liquid CO <sub>2</sub>	2.3	-20	-	-	-	-	-	-

Table 2.2 main material parameters of MEA carbon capture system -- liquid [46]

Serial number	Name	Pressure MPa	Temperature °C	Specific heat kJ·kg·K-1	Composition mol%		Enthalpy× 10 <sup>-3</sup> KW
					CO <sub>2</sub>	amine	

1	Absorption tower rich liquid	0.11	56	3.191	2.55	6.01	168.106
2	Desorption tower rich liquid	0.44	98.6	3.236	2.55	6.01	300.191
3	Desorption tower poor liquid	0.16	112	3.274	0.91	6.12	332.465
4	Heat exchanger poor liquid	0.11	69	3.203	0.91	6.12	200.380
5	Liquid poor out of cooler	0.45	40	3.195	0.91	6.12	115.872
6	Lean liquid into the absorber	0.45	40	3.195	0.91	6.12	115.647
7	Drainage	0.45	40	-	-	-	0.225
8	Desorption tower rehydration	0.40	40	4.17	-	-	4.417
9	condensate	0.6	40	4.29	-	-	4.297

## 2.2 Energy consumption analysis of a carbon capture system

The process of MEA rich liquid decomposing high concentration CO<sub>2</sub> and MEA lean liquid in the desorption tower includes the desorption reaction of the rich liquid heating up in the reboiler, releasing CO<sub>2</sub>, and exhausting the regeneration gas, so the energy consumption of the carbon capture system should be from these three. The analysis is from the aspects of sensible heat required for temperature increase of rich liquid, heat of reaction required for decomposition of rich liquid and heat taken away from exhaust of regeneration gas.

$$Q_z = Q_s + Q_r + Q_c \quad (2.5)$$

Where:

$Q_z$  — Energy consumption required for regeneration of absorbent rich liquid, kJ/h;

$Q_s$  — Sensible heat required for temperature increase of rich liquid, kJ/h;

$Q_r$  — Reaction heat required for desorption of rich liquid, kJ/h;

$Q_c$  — Heat taken away when the desorption tower discharges regeneration gas, kJ/h.

					<i>13.04.01.2020.286.YY EN</i>	<i>page</i>
						22
<i>ИЗМ</i>	<i>Page</i>	<i>Document #</i>	<i>Signat.</i>	<i>Date</i>		

The sensible heat required by the temperature rise of rich liquid is expressed as follows:

$$Q_s = c_p \cdot m_L \cdot \Delta t \quad (2.6)$$

$$m_L = K \frac{X_{CO_2} \eta}{\alpha_{CO_2}^R - \alpha_{CO_2}^L} \cdot \frac{M_a}{\Phi} \quad (2.7)$$

Where:

$c_p$  — Specific pressure heat capacity of MEA solution, , generally 4.187;

$m_L$  — Flow rate of MEA solution, ;

$\Delta t$  — Performance factor of heat exchanger, K;

K — The circulating magnification of the solution, which is between 1.1 and 2.0;

$X_{CO_2}$  — The flow rate of CO<sub>2</sub> in the flue gas,;

$\eta$  — CO<sub>2</sub> removal efficiency, 85%;

$\alpha_{CO_2}^R$  — MEA rich CO<sub>2</sub> load,;

$\alpha_{CO_2}^L$  — MEA lean CO<sub>2</sub> load,;

$M_a$  — The molar mass of the active ingredient of the absorbent in the absorbent,;

$\Phi$  — The mass fraction of the active ingredient in the absorption liquid, %.

The reaction heat required for desorption of rich liquid is expressed as follows:

$$Q_r = P_{CO_2} \cdot \Delta Q_{CO_2} = X_{CO_2} \cdot \eta \cdot \Delta Q_{CO_2} \quad (2.8)$$

Where:

$P_{CO_2}$  — CO<sub>2</sub> production,;

$\Delta Q_{CO_2}$  — Average heat of reaction required per unit CO<sub>2</sub>,;

The heat taken away when the regeneration gas is discharged:

					13.04.01.2020.286.YY EN	page
						23
ИЗМ	Page	Document #	Signat.	Date		

$$Q_c = Rr_{H_2O}P_{CO_2} = X_{CO_2}\eta Rr_{H_2O} \quad (2.9)$$

Where:

$R$  —The reflux ratio at the top of the desorption tower, in general, take 3:1~1:1;

$r_{H_2O}$  —For the latent heat of vaporization of water, take 39.

According to the above formula, the energy consumption of the carbon capture system can be obtained:

$$Q_z = K \frac{X_{CO_2}\eta}{\alpha_{CO_2}^R - \alpha_{CO_2}^L} \cdot \frac{M_a}{\Phi} c_p \cdot \Delta t + X_{CO_2} \cdot \eta \cdot \Delta Q_{CO_2} + X_{CO_2}\eta Rr_{H_2O} \quad (2.10)$$

Unit renewable energy consumption can be expressed as follows:

$$q_z = \frac{K}{\alpha_{CO_2}^R - \alpha_{CO_2}^L} \cdot \frac{M_a}{\Phi} c_p \cdot \Delta t + \Delta Q_{CO_2} + Rr_{H_2O} \quad (2.11)$$

The steam demand of carbon capture system can be obtained from the following equation:

$$D_{st} = \frac{Q_z}{\Delta H} \quad (2.12)$$

Where:

$D_{st}$  —Steam flow of carbon capture system;

$\Delta H$  —Enthalpy difference between the inlet and outlet of the reboiler supply side..

## 2.3 Thermal performance analysis of the system

### 2.3.1 Calculation of CO<sub>2</sub> emission rate from fixed combustion of coal

According to the different industrial analysis data obtained, different formulas are selected to calculate the CO<sub>2</sub> emissions from the fixed combustion of coal in coal-fired power plants [47]. Suppose that the carbon capture rate of the system is 85%, which can be calculated by the following formula.

					13.04.01.2020.286.YY EN	page
						24
ИЗМ	Page	Document #	Signat.	Date		

$$W_{gr} = W_{coal} \cdot Q_{net,ar} \cdot C_{heat} \cdot R \times \frac{44}{12} \div 1000 \quad (2.13)$$

Where:

$W_{gr}$  —CO<sub>2</sub> emission from fixed combustion of coal, t/h;

$W_{coal}$  —The amount of raw coal consumed, t/h;

$Q_{net,ar}$  —Low calorific value, kJ/kg;

$C_{heat}$  —Carbon per unit calorific value, tons of carbon per trillion joules, provided in the provincial guidelines for the preparation of greenhouse gas inventories (trial);

$R$  —The carbon oxidation rate was 98%;

1000—Unit conversion coefficient.

$$W_{coal} = 3.6 \times Q \div \eta_b \div Q_{net,ar} \quad (2.14)$$

Where:

$Q$  —Boiler heat absorption, kJ/s;

$\eta_b$  —The boiler efficiency is 0.9295.

$$C = W_{gr} \times (1 - 85\%) \div Q_{el} \div 10^6 \quad (2.15)$$

Where:

$C$  —CO<sub>2</sub> emission rate, %;

$Q_{el}$  —Power generation, MW.

### 2.3.2 Unit circulating thermal efficiency

Cyclic thermal efficiency is an important indicator to evaluate the advantages and disadvantages of the thermal system of a large-scale coal-fired power plant. Its physical meaning is the ratio of circulating work energy to circulating heat absorption. Its general formula is:

$$\eta = \frac{w}{q} \quad (2.16)$$

					13.04.01.2020.286.YY EN	page
						25
ИЗМ	Page	Document #	Signat.	Date		

$$w = h_0 + (1 - \sum_{j=1}^r \alpha_j) q_{rh} - \sum_{j=1}^z \alpha_j h_j - (1 - \sum_{j=1}^z \alpha_j) h_c \quad (2.17)$$

$$q = h_0 - h_{fw} + (1 - \sum_1^r \alpha_j) q_{rh} \quad (2.18)$$

Where:

$w$  — Work power of per unit working fluid, kW;

$q$  — Heat absorption per unit working fluid, kW;

$h_0$  — Main steam enthalpy, kW;

$h_c$  — Enthalpy of steam turbine exhaust, kW;

$h_{fw}$  — Enthalpy of boiler feed water, kW;

$q_{rh}$  — Enthalpy of working medium in reheater, kW;

$\alpha_j$  — The flow share of the  $j$  extraction port of the turbine;

$h_j$  — The enthalpy value of the  $j$  extraction outlet of the turbine;

$r$  — The number of extraction flow of steam turbine before reheating;

$z$  — The total number of steam extracted by the turbine.

Due to the addition of a carbon capture system, the steam-water cycle of the original unit is changed, and the cycle work energy per unit working fluid and the cycle heat absorption per unit working fluid will also change accordingly. The thermal efficiency calculation formula is improved as follows:

$$w = h_0 + (1 - \sum_{j=1}^r \alpha_j - \alpha_{tc})(q_{rh1} - q_{rh2}) - \alpha_{tc} h_{tc} - \sum_{j=1}^z \alpha_j h_j - (1 - \sum_{j=1}^r \alpha_j - \alpha_{tc}) h_c \quad (2.19)$$

$$q = h_0 - h_{fw} + (1 - \sum_{j=1}^r \alpha_j - \alpha_{tc})(q_{rh1} - q_{rh2}) \quad (2.20)$$

					13.04.01.2020.286.YY EN	page
						26
ИЗМ	Page	Document #	Signat.	Date		

Where:

$\alpha_{tc}$  —Reboiler inlet steam share;

$h_{tc}$  —Inlet enthalpy of reboiler, kJ/kg;

$q_{rh1}$  —The enthalpy rise of primary reheating steam, kJ/kg;

$q_{rh2}$  —The enthalpy rise of the second reheat steam, kJ/kg.

### 2.3.3 Standard coal consumption rate for power generation

The standard coal consumption rate of a power station is an important index reflecting the thermal economy of the unit. The unit is kg/(kW • h), which can be calculated by the following formula.

$$b_s = \frac{1000q_0}{q_s \eta_b \eta_p} \quad (2.21)$$

Where:

$q_0$  —Unit heat consumption rate, kJ/kg;

$q_s$  —The low calorific value of standard coal, 29271 kJ/kg;

$\eta_p$  —The pipeline efficiency is 0.99.

### 2.3.4 Unit heat consumption rate

$$q_0 = \frac{3600Q}{p_e \eta_m \eta_g} \quad (2.22)$$

Where:

$p_e$  —Generating power of the unit;

$\eta_m$  —Mechanical efficiency;

$\eta_g$  —Generator efficiency.

					<i>13.04.01.2020.286.YY EN</i>	<i>page</i>
						27
<i>ИЗМ</i>	<i>Page</i>	<i>Document #</i>	<i>Signat.</i>	<i>Date</i>		



## Chapter summary

This chapter mainly introduces the reaction mechanism and process flow of carbon capture technology based on monoethanolamine, understands the basic theory of carbon capture unit, and focuses on the derivation of the calculation formula for the energy consumption of carbon capture system regeneration. The thermal performance of the system is analyzed, and the main performance evaluation indicators and technical and economic indicators are introduced, which lays the foundation for subsequent research and comparative evaluation.

## 3 STUDY ON CHARACTERISTICS OF SOLAR ENERGY SYSTEM

### 3.1 Trough solar collector

Parabolic trough solar thermal power generation technology is the most well-developed solar thermal power generation technology. In order to accurately simulate the structural characteristics of the collector and calculate the results reflecting the performance of the collector, it is very necessary to establish an overall model of the collector. The principle of the trough solar heat collection technology is to collect the sun rays through the parabolic trough concentrating device and reflect it to the heat collecting tube of the solar receiver, so that the solar thermal energy exchanges heat with the heat collecting medium in the receiver. The heat medium is generally heat-conducting oil. The heat-conducting oil has pyrolysis property. The heat absorption temperature is generally 300 °C -400 °C. The heat radiation medium transfers the solar radiation energy to the heat collection medium in the heat collection tube through heat exchange. By absorbing solar heat to reach the final outlet temperature requirements. The heat absorbed by the solar thermal field through the heat transfer oil can be used to heat fluid for power generation systems or heat storage systems. The tracking system of the trough solar collector can control the direction of the parabolic mirror to ensure that the collector can move with the change of the sun's orientation.

The DSG trough solar collector with LS-2 steam direct cooling is selected for illustration. The method of direct steam cooling without the loss of intermediate heat transfer has greatly improved the performance of this system, so it has been widely used

					<i>13.04.01.2020.286.YY EN</i>	<i>page</i>
						28
<i>ИЗМ</i>	<i>Page</i>	<i>Document #</i>	<i>Signat.</i>	<i>Date</i>		

in recent years. Research and experiment. The main parameters are shown in Table 3.1 [48].

Table 3.1 Main parameters of LS-2 DSG trough solar collector

Parameter	Value
Collector area /m <sup>2</sup>	547
Length of absorption tube /m	99
Optical efficiency / %	73.3
Inner diameter of absorption tube /m	0.066
Outside diameter of absorption tube /m	0.07
Thermal conductivity of the absorption tube/ $w \cdot (m \cdot k)^{-1}$	54
Tube diameter of glass cover /m	0.115
Glass tube emissivity	0.9
Geometric concentration-light ratio	71:1

The thermal efficiency of the collector is expressed as follows [49] :

$$\eta = \eta_{opt} K_{\tau\alpha} - (a + cv)(T_{ab} - T_a) / I - \varepsilon_{ab} b(T_{ab}^4 - T_{sky}^4) / I \quad (3.1)$$

Where:

$\eta_{opt}$  —The optical efficiency of the collector is 73.3%;

$K_{\tau\alpha}$  —Correction factor of incidence angle;

$v$  —Wind speed, m/s;

$T_{ab}$  —Absorption tube temperature, K;

$T_{sky}$  —Atmospheric temperature, K;

$T_a$  —Ambient temperature, K;

$I$  —Direct radiation intensity, W/m<sup>2</sup>;

$\varepsilon_{ab}$  —Absorber emissivity.

					<i>13.04.01.2020.286.YY EN</i>	<i>page</i>
						29
<i>ИЗМ</i>	<i>Page</i>	<i>Document #</i>	<i>Signat.</i>	<i>Date</i>		

$$a = 1.91 \times 10^{-2} \frac{\text{W}}{\text{Km}^2}; \quad b = 2.02 \times 10^{-9} \frac{\text{W}}{\text{K}^4 \text{m}^2}; \quad c = 6.608 \times 10^{-3} \frac{\text{J}}{\text{Km}^3}.$$

The temperature of the absorption tube  $T_{ab}$  can be calculated from the fluid temperature  $T_b$  and heat transfer coefficient in the tube:

$$T_{ab} = T_b + Q_f (2\pi r L U) \quad (3.2)$$

Where:

$Q_f$  — Heat absorbed by the fluid;

$U$  — The heat transfer coefficient between the absorption fluid in the tube and the outer wall of the tube.

The correction factor of incidence angle  $K_{\tau\alpha}$  is a function of the incident Angle  $\theta$ :

$$K_{\tau\alpha} = \cos \theta + 0.00094\theta - 0.00005369\theta^2 \quad (3.3)$$

### 3.2 The selection of radiation intensity

The solar radiation intensity is constantly changing, and the solar radiation intensity will affect the efficiency of the solar collector and thus affect the thermal economy and technical economy of the integrated system. According to actual meteorological data, the total sunshine hours in China's Lhasa area (30 ° north latitude, 91 ° east longitude) are 3418 hours, of which 3174 hours are above 300W per unit area.

Table 3.2 Time distribution of direct radiation in Lhasa area [48]

Radiation intensity I(W/m <sup>2</sup> )	Hours of radiation intensity	Total radiation intensity hours
	(h)	(h)
below 200	122	3418
250	122	3296
300	302	3174
350	246	2872
400	62	2626
450	184	2564

500	302	2380
550	184	2078
600	184	1894
650	180	1710
700	430	1530
750	242	1100
800	306	858
850	370	552
900	182	182

Table 3.2 is analyzed as a chart below. Figure 3-1 shows the duration of sunshine in each radiation intensity section. It can be seen that the sunshine duration is the most when the radiation intensity is 700w/m<sup>2</sup>. According to the solar collector efficiency formula, in practice, when the solar radiation intensity is below 300w/m<sup>2</sup>, the collector efficiency drops greatly. At this point, the solar collector is out of operation, and the heat required by the reboiler of the carbon capture system is provided by the steam extraction of the coal-fired unit.

For the radiation distribution in a certain area, assuming a higher design radiation intensity is selected, the required heat collecting field area is relatively small. If the annual solar radiation intensity in the area is less than the design radiation intensity, the collector will be in Low-load operation will not only reduce the efficiency of the collector, but also not conducive to the use of the collector; assuming that the selected design radiation intensity is low, then a larger area of the heat collection field is required. In the case of radiation intensity, although the collector can be operated under the design parameters, it will cause a waste of radiation energy that exceeds the design radiation intensity. Therefore, the selection of design radiation intensity should consider the performance of solar collectors and the distribution of local solar radiation intensity.

					<i>13.04.01.2020.286.YY EN</i>	<i>page</i>
						31
<i>ИЗМ</i>	<i>Page</i>	<i>Document #</i>	<i>Signat.</i>	<i>Date</i>		

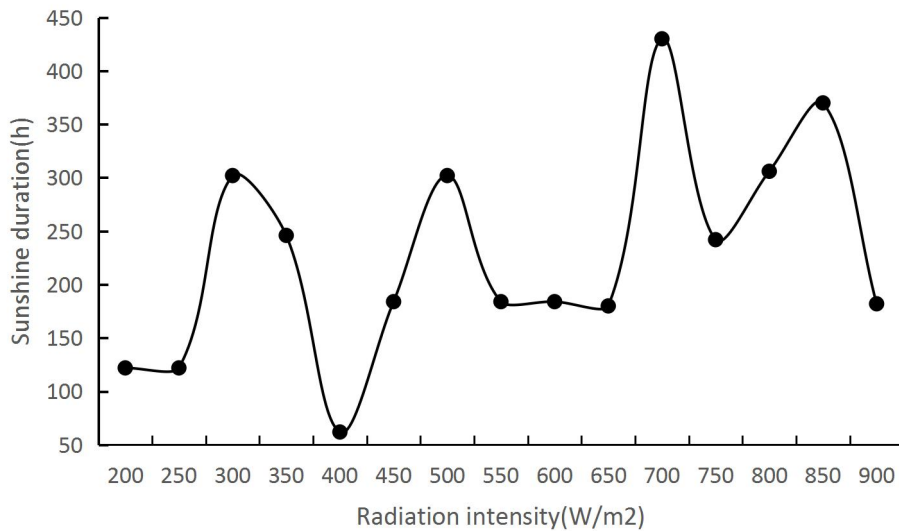


Figure 3-1 Distribution of sunshine duration in each radiation intensity section

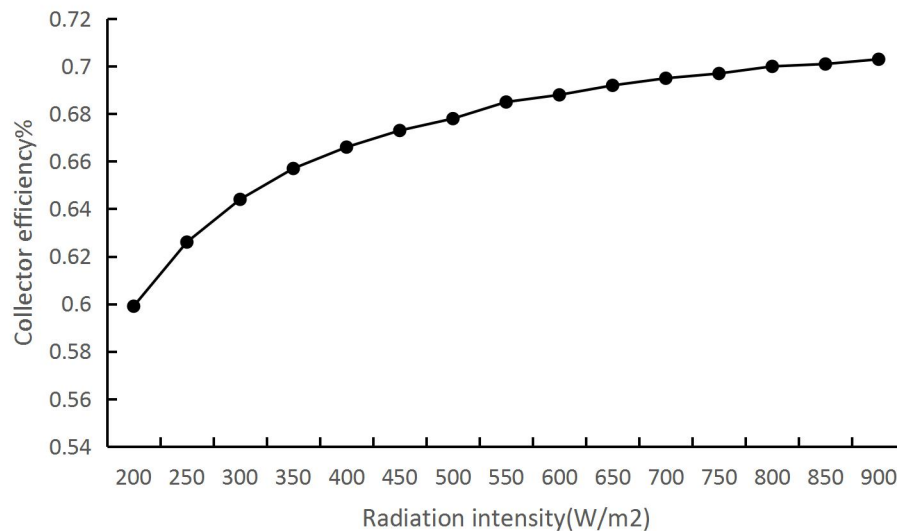


Figure 3-2 Distribution diagram of collector efficiency under different radiation intensities

Figure 3-2 as the collector efficiency map, can be seen from the graph, with the increase of the intensity of solar radiation, the collector efficiency is improving, when more than 700 w/m<sup>2</sup> solar radiation intensity, the collector efficiency of growth becomes very small, when the solar radiation intensity value is less than 400 w/m<sup>2</sup>, the efficiency of the collector down very quickly, so the best collector operation radiation intensity in 400 w/m<sup>2</sup>-700 w/m<sup>2</sup>.

### 3.3 Evaluation model of solar-assisted coal-carbon capture system

In addition to the general thermodynamic evaluation indicators mentioned in Section 2.3, the evaluation of solar-assisted coal-carbon capture system will introduce economic evaluation indicators such as Solar Photovoltaic Conversion Efficiency, Coal Saving Ratio For Investment, Average Cost Of Solar-assisted Carbon Capture and Levelized Cost of Energy to evaluate the investment value and effective utilization of solar energy.

#### 3.3.1 Solar Photovoltaic Conversion Efficiency

The photovoltaic conversion efficiency of solar energy refers to the efficiency of converting solar energy into electric energy. The higher the conversion efficiency of solar thermal power is, the higher the efficiency of the integrated system will be. It further shows that the selected scheme is the optimal scheme.

The calculation formula is as follows:

$$\eta_{\text{sol-ele}} = \frac{\Delta E}{Q_{\text{solar}}} = \frac{(E_h - m_c L \eta_{\text{ref}})}{Q_{\text{solar}}} \quad (3.5)$$

Where:

$\Delta E$  — Net generating capacity of solar farm, kW;

$m_c$  — Mass flow of standard coal per unit time, kg/s;

$L$  — Low calorific value of standard coal, 29,271 kJ/kg;

$\eta_{\text{ref}}$  — Power generation efficiency of coal-fired and carbon capture units.

#### 3.3.2 Economic evaluation index

(1) Coal saving ratio for investment

					<i>13.04.01.2020.286.YY EN</i>	<i>page</i>
						33
<i>ИЗМ</i>	<i>Page</i>	<i>Document #</i>	<i>Signat.</i>	<i>Date</i>		

The introduction of solar radiant energy will reduce the amount of coal-fired units and reduce the coal consumption, but the introduction of solar energy will inevitably increase the investment cost of solar energy collection field. In other words, the reduction of the amount of coal-fired units will be at the cost of increasing the investment of solar energy collection field. coal saving ratio of solar energy investment refers to the coal consumption that can be reduced by increasing the unit solar energy investment cost. The greater the investment coal saving ratio is, the shorter the investment recovery period of solar energy thermal collector will be [50]. Its definition is as follows:

$$\lambda = \frac{10^6 \Delta b_{cp}^s}{c_s A_m} \quad (3.6)$$

$$A_m = LW\theta \quad (3.7)$$

Where:

$\lambda$  —Coal saving ratio for investment;

$\Delta b_{cp}^s$  — The difference between the standard coal consumption of the whole plant with solar energy assisted coal-carbon capture unit and the standard coal consumption of the whole plant without solar energy assisted coal-carbon capture unit,g/kWh;

$c_s$  —Solar energy investment cost per unit area, yuan;

$A_m$  —Solar collector area,  $m^2$  ;

$L$  —Total length of solar collector, m;

$W$  —Solar collector width, m;

$\theta$  —The surplus is 1.14.

## (2) Average Cost Of Solar-assisted Carbon Capture

Average Cost Of Solar-assisted Carbon Capture (LSC-CO<sub>2</sub>) can be used to characterize the contribution of solar thermal field to the carbon capture system of solar-assisted coal-fired power plants. This index represents the investment cost of solar thermal field required to capture unit carbon dioxide [51]. The calculation formula is as follows:

					13.04.01.2020.286.YY EN	page
						34
ИЗМ	Page	Document #	Signat.	Date		

$$LSC - CO_2 = \frac{f_{cr} \cdot C_{sol} + C_{O\&M}}{M_{CO_2}} \quad (3.8)$$

Where:

$C_{solar}$  — Investment cost of solar thermal field, M\$;

$C_{O\&M}$  — Maintenance cost of solar thermal field, M\$;

$M_{CO_2}$  — Annual CO2 capture, t;

$f_{cr}$  — The average annual investment coefficient of equipment is expressed as follows:

$$f_{cr} = \frac{i(1+i)^n}{(1+i)^n - 1} \quad (3.9)$$

Where:

$i$  — The interest rate of the debt is 8%;

$n$  — Equipment service life, years.

### (3) Levelized Cost of Energy (LCOE)

The levelized cost of energy (Levelized Cost of Energy) is the power generation cost calculated after leveling the cost and power generation in the project life cycle, that is, the current value of the cost in the life cycle / the current power generation in the life cycle value. LCOE can help measure the long-term value of the system, estimate the life cycle cost of the system, and play a guiding role in project construction. The calculation formula is as follows [52]:

$$LCOE = \frac{I_0 + \sum_{t=1}^T (M_t + MEA_t + Fuel_t) \cdot (1+r)^{-t}}{\sum_{t=1}^T E_t \cdot (1+r)^{-t}} \quad (3.10)$$

Where:

$I_0$  — Initial fixed investment cost, M\$;

$M_t$  — Unit operation and maintenance cost in year t (4% of fixed investment cost in this paper), M\$;

					13.04.01.2020.286.YY EN	page
						35
ИЗМ	Page	Document #	Signat.	Date		



$MEA_t$ —MEA cost in year t, M\$;

$Fuel_t$ —Fuel cost in year t, M\$;

$E_t$ —Generating capacity in year t, MW;

$r$ —The discount rate is 5%;

$T$ —The life cycle is set to 30 years.

## Chapter summary

(1) This chapter briefly introduces the basic principle of the trough solar collector and the main parameters of the LS-2 DSG trough solar collector, and explains the efficiency expression of the collector.

(2) Taking the Lhasa area in China as an example, the distribution of solar radiation time in Lhasa area is analyzed based on actual meteorological data, and the selection principle of solar radiation intensity is mainly introduced with the method of graph analysis.

(3) On the basis of general thermodynamic evaluation indicators, three evaluation indicators are introduced to evaluate the value of solar energy, such as the solar photovoltaic conversion efficiency to evaluate the effective utilization of solar energy, the coal-saving ratio of investment, the average solar carbon capture cost and the levelized cost of energy .

## 4 MODELING AND SIMULATION OF COAL-FIRED UNIT CARBON CAPTURE SYSTEM

EBSILON software is a software tool developed by the German STEAG power company in its practical application of the power business for decades. It is a general thermodynamic modeling configuration software, which is mainly used for calculation and simulation of the thermal balance of thermal systems. The software is widely used in the design, optimization, transformation and operation of thermal power systems in power stations. In the design stage of the power station, various schemes can be

					<i>13.04.01.2020.286.YY EN</i>	<i>page</i>
						36
<i>ИЗМ</i>	<i>Page</i>	<i>Document #</i>	<i>Signat.</i>	<i>Date</i>		

designed to optimize the parameters of the scheme and simulate the operation under varying conditions; the software has advanced modular design concepts, intuitive visual interface, sufficient working materials, and sufficient material library authority, etc. Boiler modules and solar modules. This paper takes a 1000MW secondary reheat ultra-supercritical coal-fired power plant as the research object, uses EBSILON software to simulate and verify the accuracy and rationality with the power plant source data. Then the solar energy-assisted coal-fired power plant carbon capture system is simulated to find the optimal coupling scheme.

#### 4.1 Modeling and validation of coal-fired units

Taking a 1000MW unit as the research object, the unit uses secondary reheat technology, the unit type is N1000-31 / 600/610, the design rated main steam pressure is 31Mpa, the main steam / primary / secondary reheat steam temperature is 600/610 610 °C. The design rated output power of the steam turbine generator set is 1000MW, and the maximum output VWO working condition is 1074MW. The thermal system is shown in Figure 4.1, and the main parameters of the unit are shown in Table 4.1.

Table 4.1 main parameters of 1000MW coal-fired units

Parameter	Value	Unit
Unit power (VWO)	1074.467	MW
Main steam flow	2629.54	t/h
Main steam temperature	600	°C
Main steam pressure	31.8	MPa
Primary reheat steam temperature	610	°C
Primary reheat steam pressure	10.917	MPa
Secondary reheat temperature	610	°C
Secondary reheat pressure	3.323	MPa
The heat consumption rate	7063	kJ/(kW·h)
Exhaust steam pressure	0.01	MPa
Unit circulating thermal efficiency	51.17	%

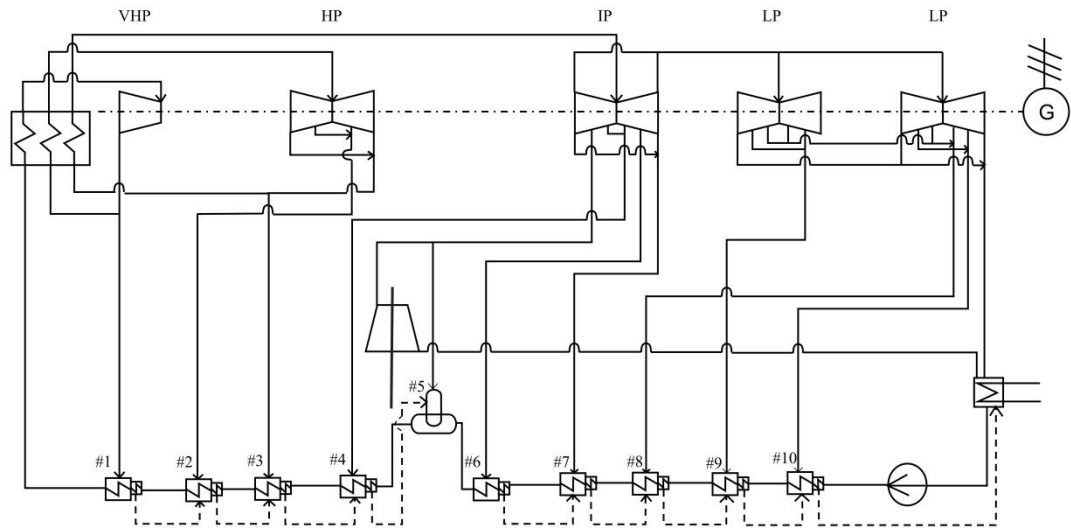


Figure 4.1 Thermal system of 1000MW coal-fired unit

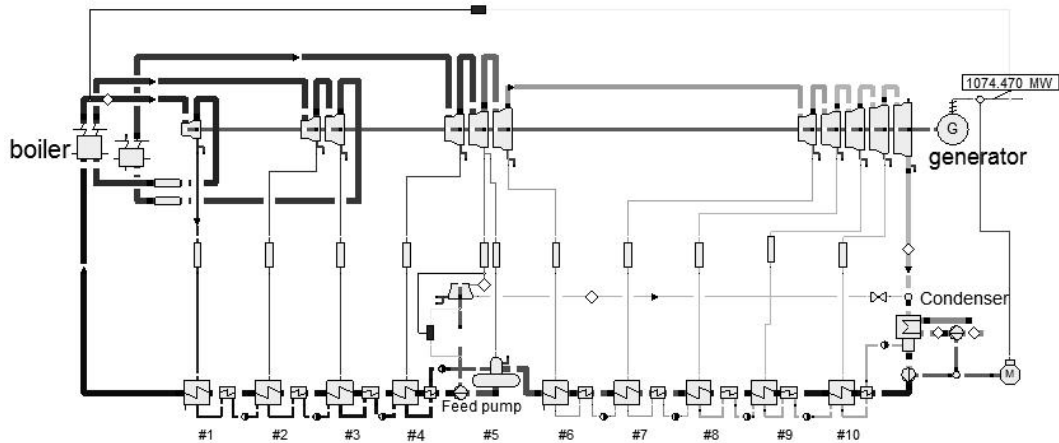


FIG. 4.2 Schematic diagram of the simulation of a coal-fired unit

This chapter establishes the thermal system model of the 1000MW boiler steam turbine system. The thermal system model of the coal-fired unit can be simulated and simulated by the EBSILON software. According to the location of the extraction point, the steam turbine is divided into twelve stages, of which the ultra-high pressure cylinder is one stage. Two-stage high-pressure cylinder, four-stage medium-pressure cylinder, five-stage low-pressure cylinder, the schematic diagram of the simulation of coal-fired units is shown in Figure 4.2.

After inputting the unit parameters into the EBSILON model, the thermal balance of the system can be simulated and calculated. The comparison between the simulated value and actual value of the main steam parameters is shown in Table 4.2. It can be seen from the table that the simulated value is not much different from the design value

(the shaft seal leakage is not considered), and it can be considered that the calculation result of the model is sufficient to reflect the actual operation of the unit.

Table 4.2 Comparison of simulated and actual steam parameters of coal-fired units

	Pressure(MPa)		Temperature(°C)		Flow rate(kg/s)	
	Actual value	Simulation value	Actual value	Simulation value	Actual value	Simulation value
Main steam parameter	31.80	31.80	600.00	600.00	752.80	742.72
Reheat steam inlet	11.67	11.42	431.20	429.63	699.10	705.61
Reheat steam outlet	10.92	10.92	610.00	610.00	699.10	705.61
Secondary reheat steam inlet	3.70	3.72	434.10	434.33	600.17	615.04
Secondary reheat steam outlet	3.32	3.32	610.00	610.00	600.17	615.04
Primary extraction	11.67	11.42	431.20	429.63	747.01	742.72
Secondary extraction	6.67	6.67	527.50	527.55	59.13	48.65
Third extraction	3.70	3.72	434.20	434.33	642.37	656.96
4th extraction	1.95	1.95	526.40	526.45	21.86	13.35
5th extraction	1.16	1.16	446.50	446.49	54.26	58.95
6th extraction	0.81	0.81	393.54	393.65	21.98	23.06
7th extraction	0.44	0.43	312.70	312.59	32.45	32.70
8th extraction	0.14	0.14	193.66	193.70	7.59	19.07
9th extraction	0.07	0.07	117.91	117.92	21.44	20.68
10th extraction	0.02	0.02	64.30	64.30	23.74	24.47
Exhaust steam	0.01	0.01	28.96	28.96	419.49	422.77

## 4.2 Model establishment of carbon capture system for coal-fired units

### 4.2.1 Research on coupling scheme

The 1000MW coal-fired unit established in section 4.1 is used as the reference unit, and the post-combustion carbon capture technology is applied for carbon dioxide capture on the basis of the reference unit. The post-combustion carbon capture

					<i>13.04.01.2020.286.YY EN</i>	<i>page</i>
						39
<i>ИЗМ</i>	<i>Page</i>	<i>Document #</i>	<i>Signat.</i>	<i>Date</i>		

technology is relatively mature and has a small impact on the existing power plants with high flexibility. The carbon dioxide content of the flue gas with large flow is not very high after treatment, and chemical absorption method is more suitable for large coal-fired power plants. Among various chemical absorbents, alcohol-amine absorbents, especially MEA, are widely used due to their maturity, stability, rapid reaction rate and high recovery capacity. Carbon capture based on alcohol amine solution (MEA) is one of the most common and frequently used methods. For the integrated coal-capture system, if all the energy required for liquid-rich desorption in the carbon capture system is provided by coal-fired units, the performance of the original system will be affected. In addition to the huge energy penalty of the carbon capture system, the location of the steam source, namely where the steam is taken from and the location of the water back should also be considered. The steam quality provided by each suction port is not the same, and the selected locations of the suction and return water are different, which have different influences on the performance parameters of the whole system. Therefore, it is particularly important to select the appropriate suction location for the system integration.

Based on the high temperature degradation characteristics of MEA solution, the temperature of the rich liquid in the reboiler is generally controlled at about 122 °C. If the heat exchange end difference of the reboiler is set to 10 °C, the inlet steam temperature should be 132 °C, the corresponding saturated steam pressure It is 0.287MPa. Table 4-3 shows the main process parameters of the carbon capture system.

Table 4-3 Parameters of carbon capture system [53]

Parameter	Value	Unit
The temperature of flue gas inlet absorption tower	40	°C
The temperature of lean liquid inlet absorption tower	40	°C
Heat transfer difference of reboiler	10	°C
The temperature of the steam inlet reboiler	132	°C
The pressure of the steam inlet reboiler	0.287	MPa
Energy consumption of per unit CO <sub>2</sub> regeneration	3.8	GJ/t
CO <sub>2</sub> removal rate	85	%

This chapter provides six different steam supply schemes for carbon capture of a 1000MW secondary reheat coal-fired power plant, from the primary reheat cold section (Scheme A) and the hot section (Scheme B), the secondary reheat cold section (Scheme C) and the hot section (Scheme D), the middle and low pressure cylinder pipeline connection (Scheme E), and the middle and low pressure cylinder pipeline connection where there is no small back pressure machine (Scheme F) . Two aspects should be considered in the selection of the extraction port: one is the steam temperature of the extraction port, and the other is that the flow rate should meet the requirements of the carbon capture system [54]. After the analysis of the superheat of each extraction outlet of the thermal system mentioned in Section 4-1, found that after the first and second reheat, the #2 and #3 extraction outlet of the high-pressure cylinder and the #4, #5 and #6 of the medium pressure cylinder have high steam superheat.

In view of the problem of excessive superheat of steam extraction after reheating of the unit, the addition of a carbon capture turbine to the unit is considered to have less disturbance [55]. adopts the way of adding small steam turbines, so that the superheated extraction steam first expands in the small steam turbine to do work, consumes most of the superheat, and then enters the reheat heater to heat the feed water [56]. The specific steam supply thermal system diagram is shown in Figure 4.3-Figure 4.8.

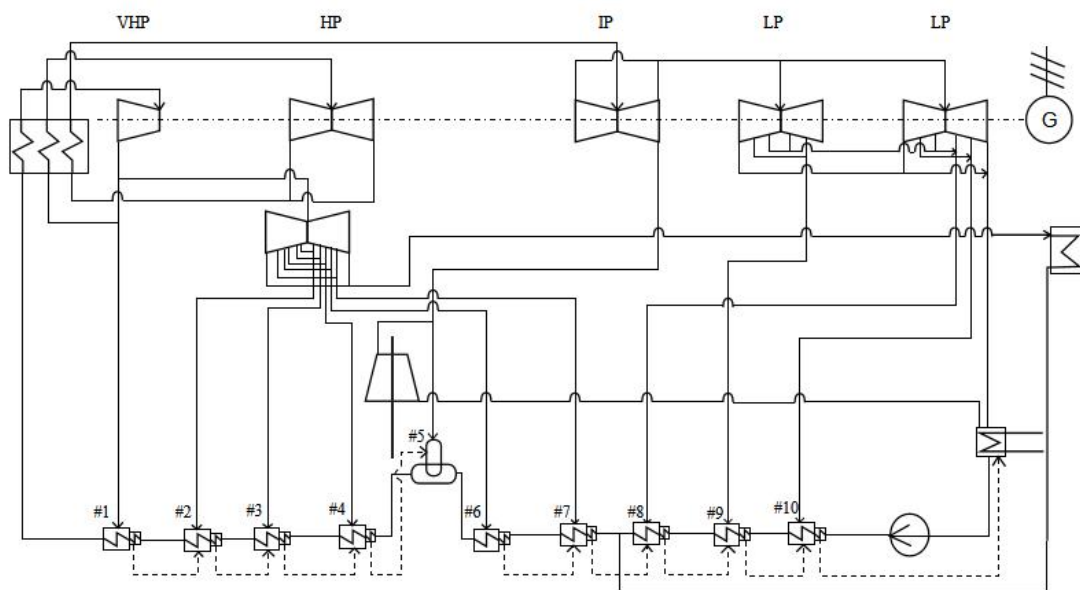


FIG. 4.3 Plan A -steam come from the cooled section of reheating

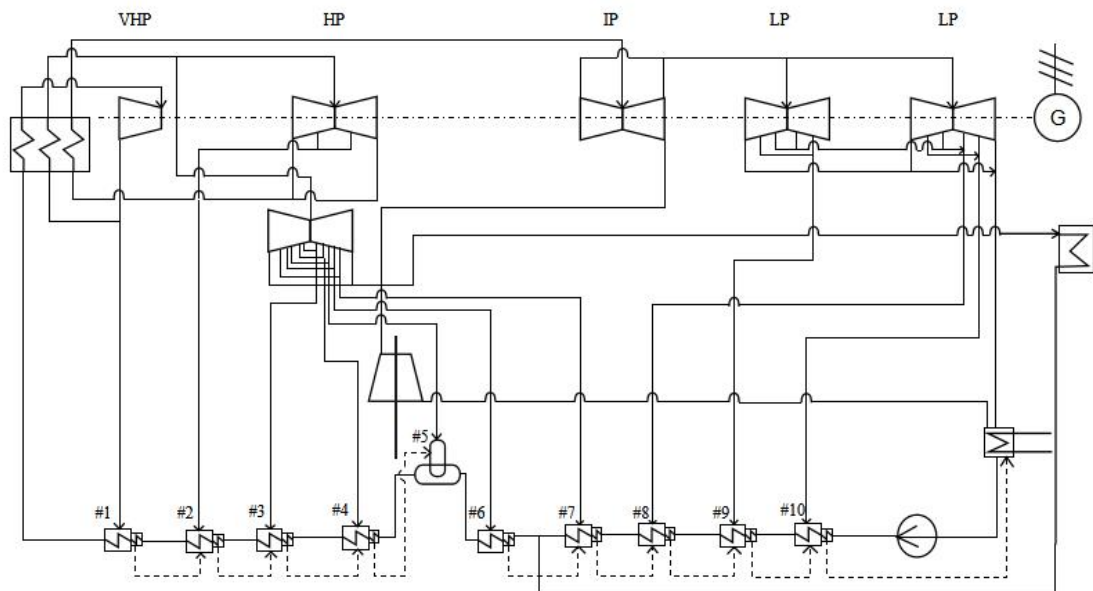


Figure 4.4 Plan B-steam come from the hotted section of reheating

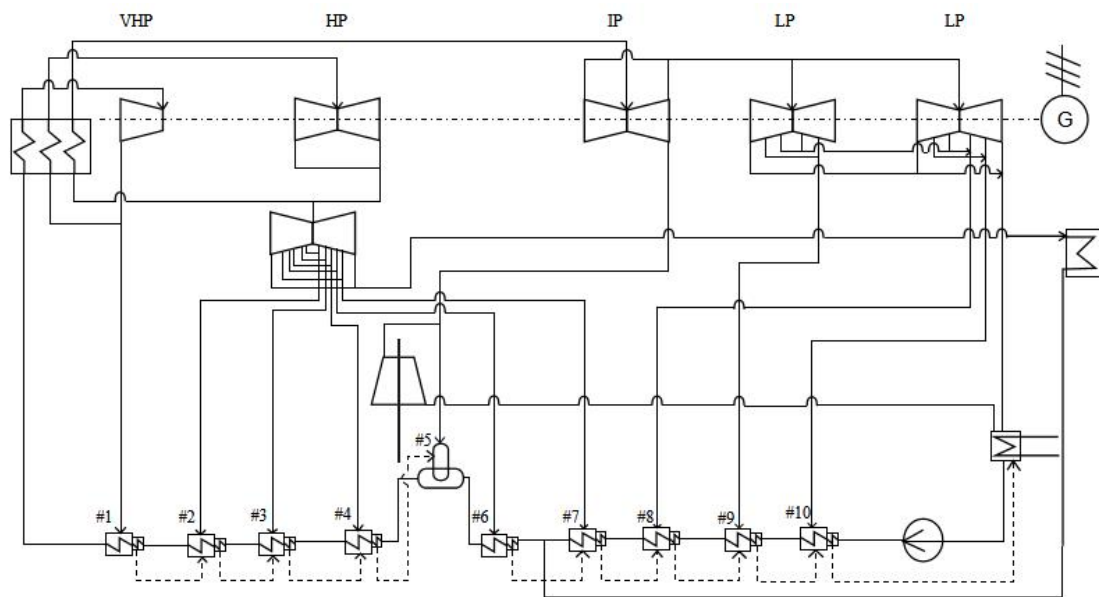


Figure 4.5 Plan C-steam come from the cooled section of secondary reheating

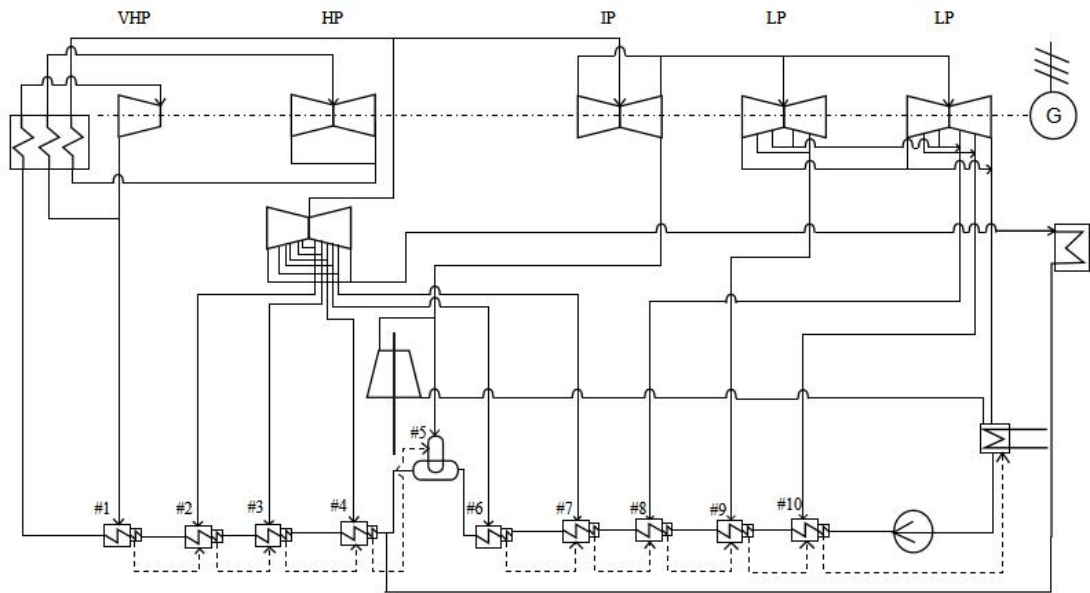


FIG. 4.6 Plan D-steam come from the hotted section of secondary reheating

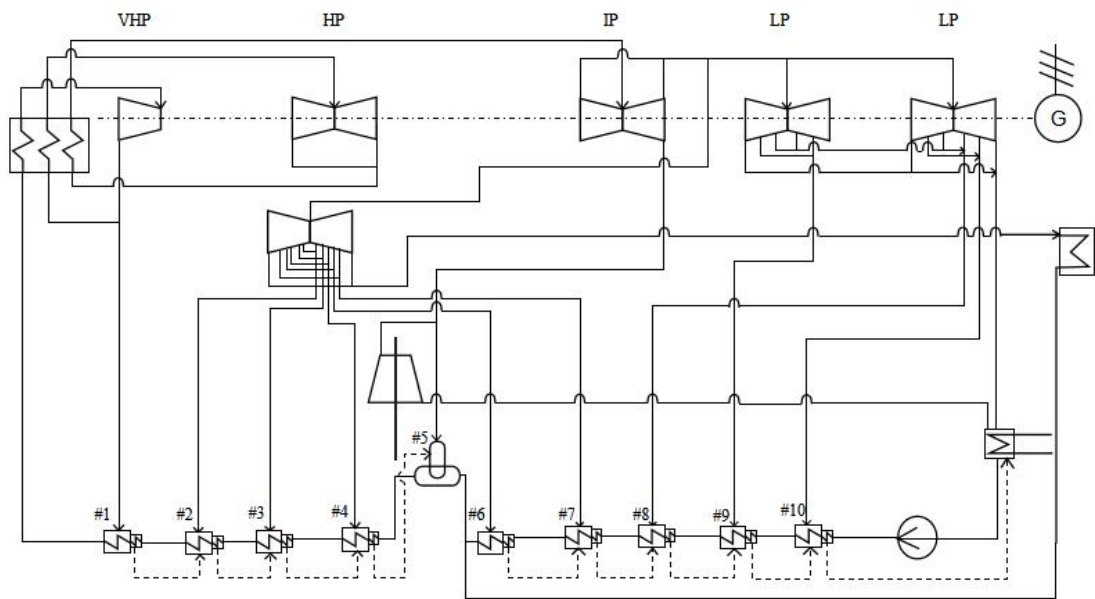


FIG. 4.7 Plan E-steam come from the pipeline connection of middle and low pressure cylinder



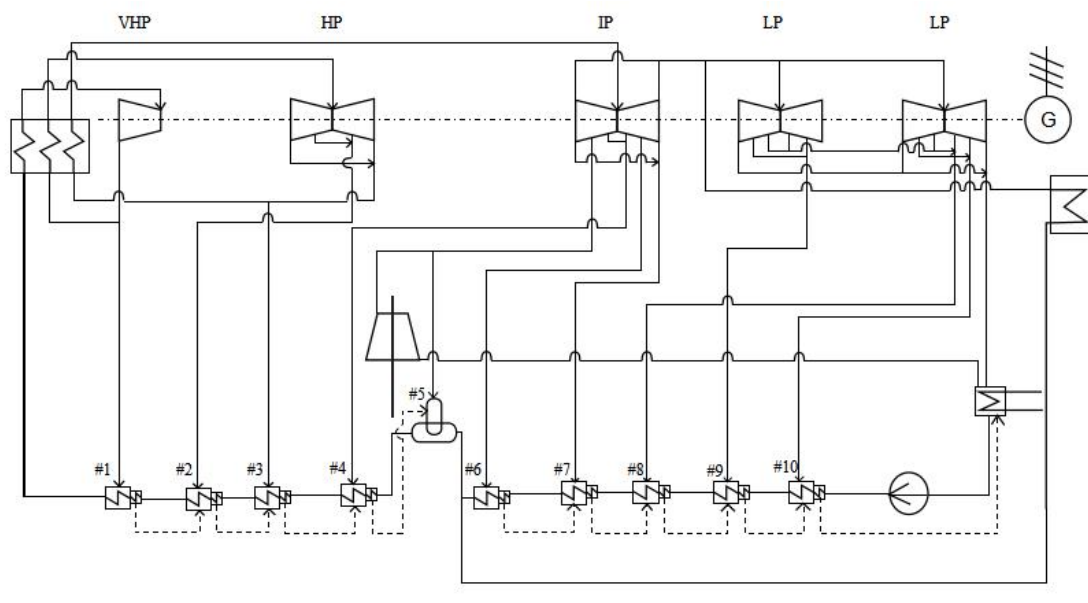


FIG. 4.8 Plan F-non-carbon capture steam turbine & steam come from the pipeline connection of middle and low pressure cylinder

#### 4.2.2 Results analysis

According to the six steam supply schemes shown above, after the EBSILON simulation calculation, the thermal evaluation index values are obtained, as shown in Table 4-4. Among the six steam supply schemes, it can be seen that when scheme C supplies steam from the secondary reheat cooling section, the circulating thermal efficiency of the unit is the highest of the six steam supply schemes, which is 44.06%, and the CO<sub>2</sub> emission rate is the lowest, as low as 122.06g / (kW·h), the standard coal consumption rate and heat consumption rate of power generation are the lowest, which is the optimal scheme for the coupling of coal-carbon capture system.

Table 4.4 Comparison of thermal performance of six steam supply methods

Plan	Circulating thermal efficiency %	CO <sub>2</sub> emission rate g/(kW·h)	Standard coal consumption g/(kW·h)	Unit heat consumption rate kJ/(kW·h)	Power plant heat consumption rate kJ/(kW·h)
A	44.04	122.09	315.77	8511.91	9241.90
B	43.88	122.54	316.92	8543.15	9275.83

C	44.06	122.06	315.67	8509.43	9239.22
D	43.74	122.93	317.93	8570.19	9305.19
E	43.48	123.67	319.83	8621.52	9360.92
F	42.59	126.25	326.51	8801.51	9556.35

Optimal solution C. The standard coal consumption rate of power generation by the secondary reheating and cooling section steam supply is 10.74g / (kWh) lower than that of the program F without additional small back pressure machine, and the CO<sub>2</sub> emission rate is 4.19g / (kWh) lower than that of the program F . Scheme F has the lowest cycle thermal efficiency, and the highest coal consumption rate, heat consumption rate and carbon dioxide emission rate. This shows that the addition of a small back pressure machine can effectively improve the energy utilization efficiency.

Table 4.5 Comparison of main parameters of coal-fired and coal-carbon capture systems

Parameters	Coal-fired unit	Coal-carbon capture unit	Unit
Unit output power	1074.47	854.44	MW
Cyclic thermal efficiency	51.17	44.06	%
Power generation standard coal consumption rate	268.5	315.67	g/(kW · h)
Heat consumption rate	7292.12	8340.1	kJ/(kW · h)
Secondary reheat steam parameters	3.04/434.68/594.11	2.55/423.99/230.77	Mpa/°C/kg/s
CO <sub>2</sub> emission rate	700.65	122.06	g/(kW · h)

It can be seen from Table 4-5 that after adding a carbon capture device to the coal-fired system, the energy penalty is huge, the total power of the system decreases by 220.03MW, and the circulating thermal efficiency decreases by 7.11 percentage points. 363.34kg / s is extracted from the high-pressure cylinder extraction steam, and nearly 61% of the steam is used to provide the regeneration energy consumption of the carbon capture unit reboiler, because the high-pressure cylinder extraction steam parameters are much higher than the steam parameters required by the reboiler Therefore, the scheme of adding a carbon-capturing turbine was adopted to recover part of the heat energy and make up for a part of the energy loss. At the same time, the temperature and pressure of

					<i>13.04.01.2020.286.YY EN</i>	<i>page</i>
						45
<i>ИЗМ</i>	<i>Page</i>	<i>Document #</i>	<i>Signat.</i>	<i>Date</i>		

the extracted steam from the high-pressure cylinder were reduced to meet the needs of the reboiler.

**Chapter summary**

This chapter is mainly about modeling and analysis of integrated systems, taking 1000MW secondary reheating unit as the research object, and using heat balance simulation software EBSILON to establish the simulation model. Input the unit parameters into the EBSILON model, and perform thermal balance simulation calculation on the system. By comparing the simulated value of the main steam parameters with the actual value, it is concluded that the simulated value is not much different from the design value, and the calculation result of the model is sufficient to reflect the actual operation of the unit. Taking the established 1000MW coal-fired unit as a reference unit, the post-combustion carbon capture technology is used to capture carbon dioxide on the basis of the reference unit, and the steam extraction of the original coal-fired unit is used to provide a heat source for rich liquid regeneration. In addition to considering the huge energy penalty of the carbon capture system, the location of the steam source and the location of the return water are also considered. To this end, six different steam supply schemes were proposed for carbon capture of a 1000MW secondary reheat coal-fired power plant, from the primary reheat cold section (Scheme A) and the hot section (Scheme B), to the secondary reheat cold section (Scheme C) and the hot section (scheme D), medium and low pressure cylinder pipeline connection (scheme E), and the scheme of the medium and low pressure cylinder pipeline connection where there is no small back pressure machine compared with the addition of small back pressure machines in the medium and low pressure cylinder pipeline connection Option F). After the simulation results are obtained, the results are analyzed to find the optimal coupling scheme. The results show that: Of the six coal-carbon capture and steam supply schemes proposed in this chapter, scheme C is the steam supply from the secondary reheating and cooling section, the unit's circulating thermal efficiency is the highest, 44.06%, and the CO<sub>2</sub> emission rate is the lowest. As low as 122.06g / (kWh), the standard coal consumption rate and heat consumption rate of power generation are the lowest, which is the best plan. The scheme without a small back pressure machine has the lowest cycle thermal efficiency and the highest coal consumption rate, heat consumption rate and carbon dioxide emission rate. It can be

					<i>13.04.01.2020.286.YY EN</i>	<i>page</i>
						46
<i>ИЗМ</i>	<i>Page</i>	<i>Document #</i>	<i>Signat.</i>	<i>Date</i>		

seen that the addition of a small back pressure machine can effectively improve the energy utilization efficiency.

## **5 PERFORMANCE ANALYSIS OF THE CARBON CAPTURE SYSTEM FOR SOLAR ENERGY ASSISTED COAL-FIRED UNITS**

In the previous chapter, the characteristics of the solar-assisted coal-fired unit carbon capture technology have been analyzed. The performance and parameters of the trough solar energy and the selection of radiation intensity have been introduced. The next step is to model the thermodynamic system of the integrated system. The integration method, namely the integration of solar energy and high-pressure recuperation system, is denoted as scheme I ; the integration of solar energy and low-pressure heat-regeneration system is denoted as scheme II ; the integration of solar energy and carbon capture system is denoted as scheme III. In the previous section, we analyzed six schemes for coupling coal-burning and carbon capture, and obtained scheme C, that is, taking steam from the secondary reheating and cooling section as the optimal scheme. The three complementary integration methods are all modeled based on scheme C.

### **5.1 Study on integrated system scheme**

#### (1) Solar energy supplies energy to the high-pressure heater

The solar energy is integrated with the high-pressure heater, and the radiant energy collected by the solar heat collection field is used to heat the heat transfer medium heat transfer oil, and the energy of direct solar radiation is transferred to the heat collection medium in the metal tube. The heat collection medium absorbs the solar radiation energy and reaches the final outlet temperature requirement, then exchanged with some of the feed water in the high-pressure heater of the steam turbine to replace the high-extracted steam extraction of the coal-fired unit steam turbine, and the replaced steam extraction can continue to do work in the steam turbine to increase the unit output. To make up for part of the energy consumption. Figure 5.1 is a schematic diagram of the solar energy instead of high-pressure heater to do work.

					<i>13.04.01.2020.286.YY EN</i>	<i>page</i>
						47
<i>ИЗМ</i>	<i>Page</i>	<i>Document #</i>	<i>Signat.</i>	<i>Date</i>		

(2) Solar energy supplies energy to the low-pressure heater

The condensed water from the condenser is divided into two parts, one part is heated by the original regenerative system, the other part is drawn into the solar heat collecting field, and after being heated, it is returned to the low pressure heater according to the principle of temperature equalization. The heat collecting field replaces the low-pressure heaters No. 7, No. 8, No. 9, and No. 10 to heat part of the condensed water, and the replaced steam can continue to do work in the low-pressure cylinder of the steam turbine. Figure 5.2 is a schematic diagram of the solar energy instead of low-pressure heater to do work.

In the integration of solar energy and heat recovery system, the feed water is divided into two parts, part of the feed water enters the boiler through the original heat recovery system, and part of it enters the solar heat collecting field for heat exchange. The share of feed water entering the solar heat collector field is different, but the temperature and pressure of the fluid outlet after heat exchange in the heat collector field can be calculated, and the feed water heated by the solar heat collector field is returned according to the principle of temperature equalization and energy balance into the corresponding heater.

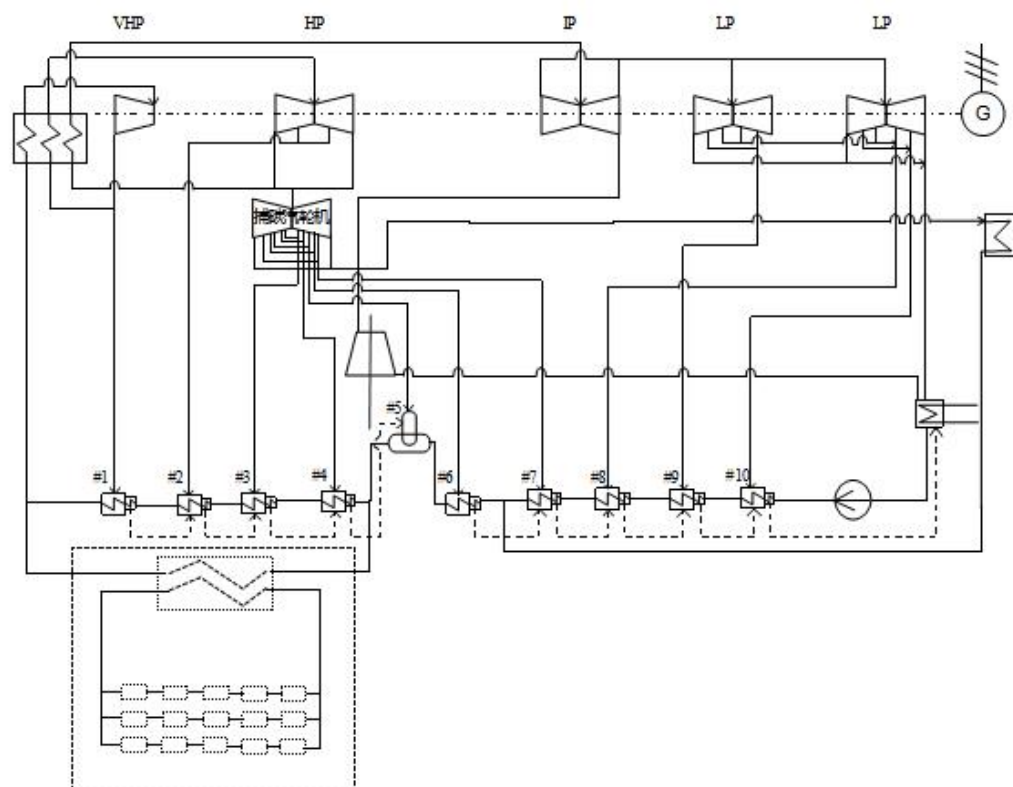


Figure 5.1 scheme I Schematic diagram of solar energy replacing high-pressure heater

					13.04.01.2020.286.YY EN	page
						48
ИЗМ	Page	Document #	Signat.	Date		

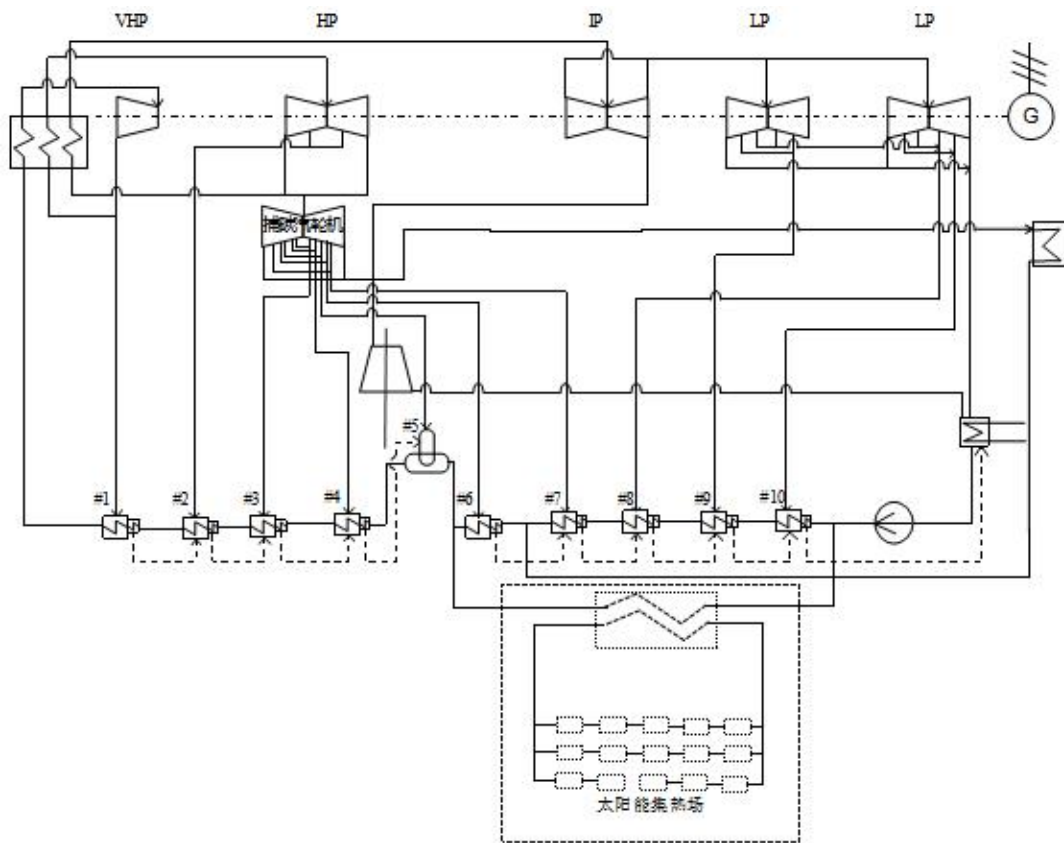


Figure 5.2 scheme II Schematic diagram of solar energy replacing low-pressure heater

(3) Solar energy supplies energy to the carbon capture system

Solar energy provides energy to the carbon capture system by directly using the heat collected by the solar heat collector to provide the energy consumed by the carbon capture system. After the steam condensed in the reboiler is divided into two parts, one part enters the unit's regenerative system supplies the boiler with water, and the other part is heated by the solar heat collecting field to provide energy for the carbon capture system reboiler desorption. At the same time, the unit's steam extraction is used as a backup heat source for the carbon capture system: when the solar radiation intensity at or above the optimal design intensity, and the heat energy provided by the solar collector can meet the energy required by the carbon capture reboiler, the energy consumption of the carbon capture system is entirely provided by the solar collector field; when the solar radiation intensity is lower than the design radiation intensity and the heat provided by the solar collector is insufficient to meet the energy required by the reboiler, the insufficient part is provided by the steam extraction of the coal-fired unit to ensure the normal operation of the carbon capture system. The schematic diagram of

solar energy directly supplying energy to the carbon capture system is shown in Figure 5.3.

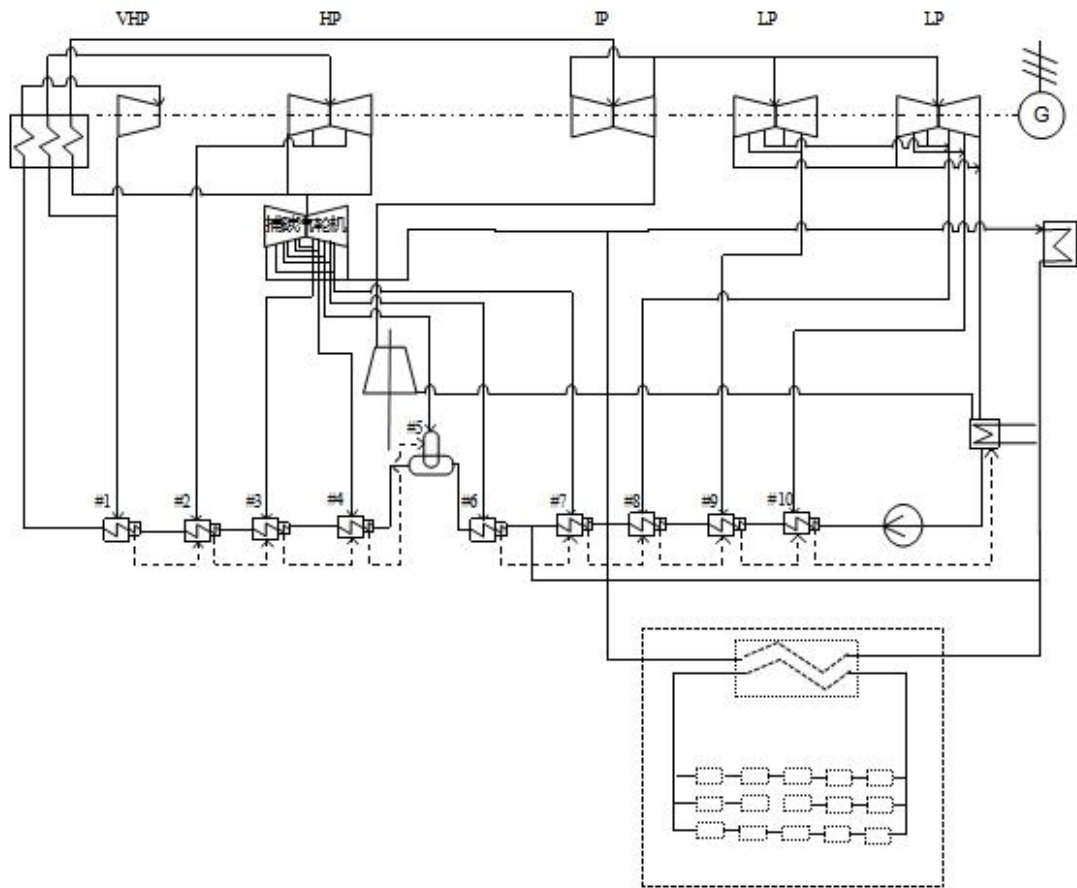


Figure 5.3 Scheme III Schematic diagram of solar energy carbon capture system

Using EBSILON heat balance software to simulate each integrated scheme, during the simulation, the main steam flow is unchanged, and the heat absorption of the boiler is basically unchanged. Due to the introduction of heat from the solar thermal field, the steam extraction of the steam turbine is reduced, and the functional capacity is increased accordingly. As the thermodynamic parameters of the coal-fired carbon capture unit change, the thermal economy of the unit will also change. The following is a schematic diagram of the simulation of the three options.

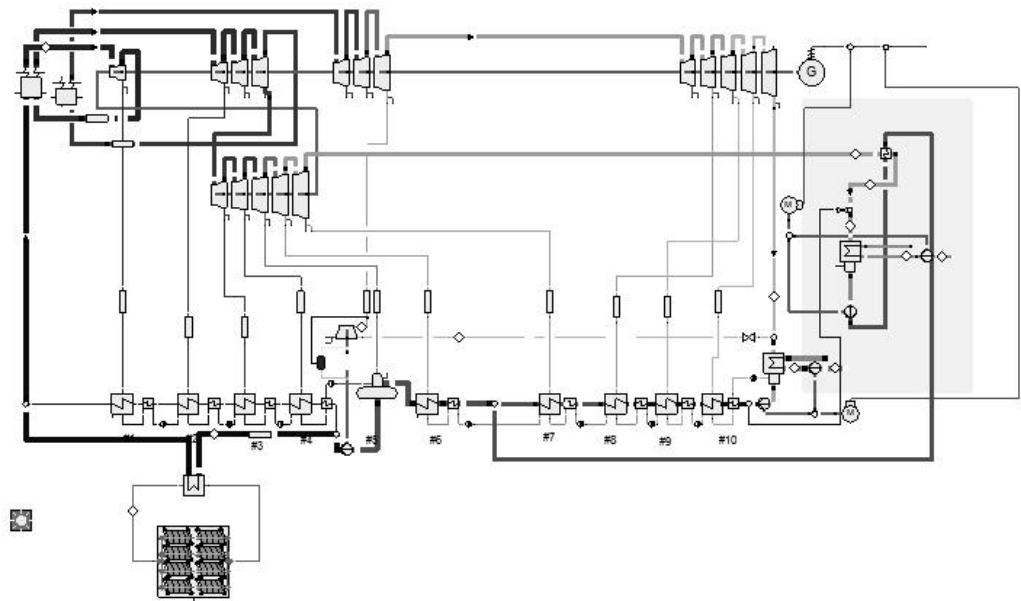


Figure 5.4 Scheme I Schematic diagram of solar energy instead of high-pressure heater simulation

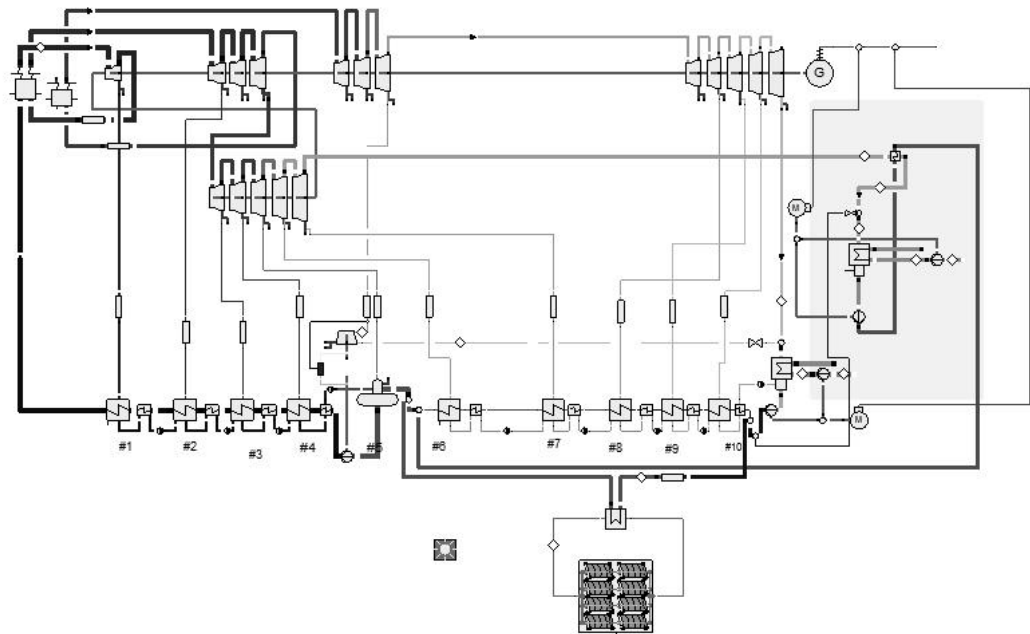


Figure 5.5 Scheme II Simulation diagram of solar energy instead of low-pressure heater



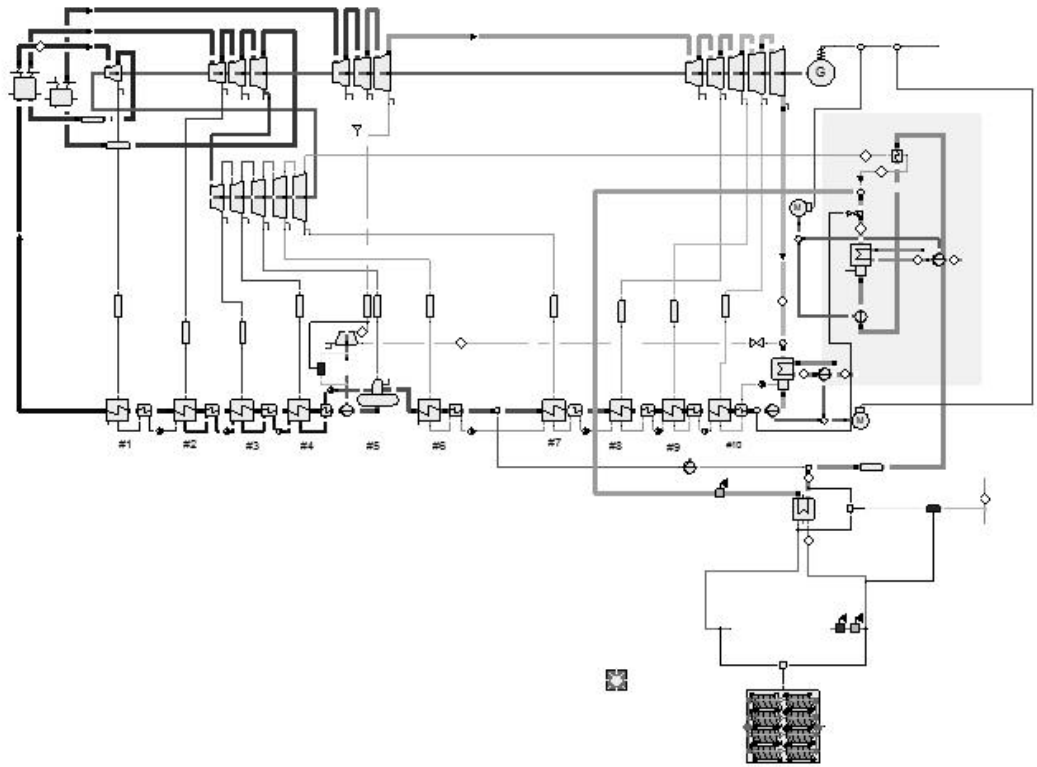


Figure 5.6 Scheme III Schematic diagram of solar energy carbon capture system simulation

## 5.2 Thermal performance comparison

According to the above three integration methods, the CO<sub>2</sub> emission rate, coal consumption rate and circulating thermal efficiency of the integrated system can be calculated by EBSILON. Based on the principle of saving investment cost, the minimum area of the solar energy collection field that can maximize the solar radiant energy is selected. The direct solar radiation intensity is 700w/m<sup>2</sup>. According to different schemes, adjust the feed water flow rate and outlet temperature of the solar collector. After EBSILON simulation calculation, the values of each thermal evaluation index are obtained, as shown in Table 5.1.

					<i>13.04.01.2020.286.YY EN</i>	<i>page</i>
						52
<i>ИЗМ</i>	<i>Page</i>	<i>Document #</i>	<i>Signat.</i>	<i>Date</i>		

Table 5.1 Comparison of thermal performance of three integrated mode

Plan	Circulating thermal efficiency %	CO <sub>2</sub> emission rate g/(kW·h)	Standard coal consumption g/(kW·h)	Unit heat consumption rate kJ/(kW·h)	Power plant heat consumption rate kJ/(kW·h)
I	53.65	100.23	259.22	6987.54	7586.81
II	44.81	119.99	310.32	8365.26	9082.68
III	50.83	105.78	273.57	7374.61	8007.07

It can be seen intuitively

from Figures 5-7 that the standard coal consumption rate and CO<sub>2</sub> emission rate of coal-carbon capture schemes I, II, and III with solar energy assistance are lower than those without coal-fired coal-carbon capture scheme. C. It shows that the use of solar energy can effectively reduce the amount of coal burned. Among the three schemes, the thermal efficiency of scheme I is the highest, and at the same time, the CO<sub>2</sub> emission rate, coal consumption rate and heat consumption rate are the lowest. Compared with scheme II, scheme I has a coal consumption 51.1g / (kWh) lower than scheme II, CO<sub>2</sub> emission is 19.76g / (kWh) lower than scheme II, and the cycle thermal efficiency is 8.84 percentage points higher than scheme II; The coal consumption is 14.35g / (kWh) lower, the CO<sub>2</sub> emission rate is 5.55g / (kWh) lower, and the thermal efficiency is 2.82 percentage points higher, which is the best thermal performance among the three schemes. The integration method of solar energy coupled with the high heat recovery system is better than that of the solar energy directly supplying energy to the carbon capture system.

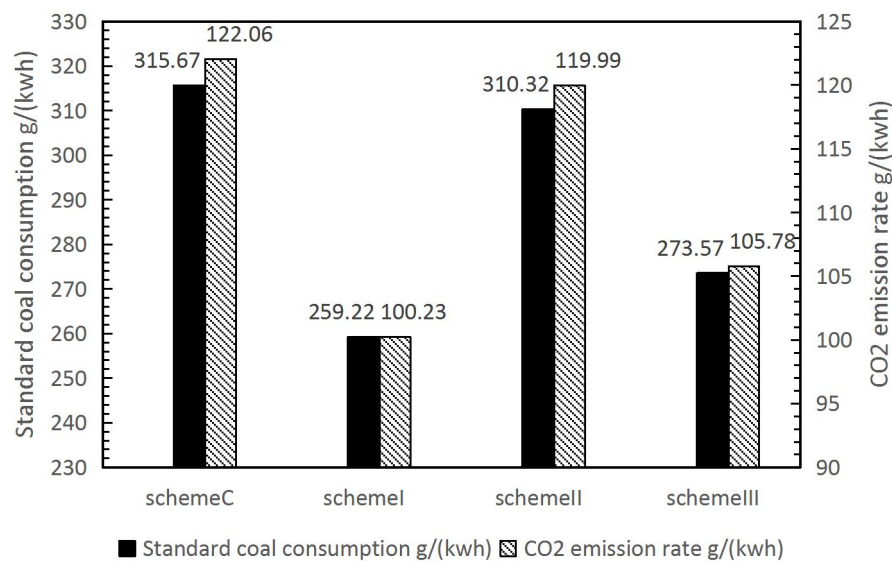


Figure 5.7 Comparison of coal consumption rate and CO<sub>2</sub> emission rate of Plan I, Plan II, Plan III and Plan C

Table 5.2 Solar photovoltaic conversion efficiency parameters

Project	Scheme I	Scheme II	Scheme III
Total power generation of solar-assisted coal-carbon capture unit /MW	1091.889	871.425	1043.045
Total power generation capacity of coal-carbon capture unit without solar energy assistance / MW	854.442	854.442	854.442
Heat absorption of solar field /MW	492.831	95.582	659.361
Solar photovoltaic conversion efficiency %	48.18%	17.77%	28.60%

Obtained from table 5.2, after the introduction of solar thermal field, the system's power unit is higher than without solar assisted, among them, the scheme I higher than without carbon capture of solar energy auxiliary units of 237.447 MW, scheme III higher than without carbon capture of solar energy auxiliary units of 188.603 MW, scheme I higher than the scheme III 48.844 MW. Solar photoelectric conversion efficiency: scheme I > scheme III > scheme II, scheme I nearly 20% higher than the schemes III and solar energy conversion of the visible scheme I effect is best, the solar energy heat utilization is more reasonable.

Table 5.3 Coal-fired units with coal - carbon capture unit and coal - carbon capture unit scheme I of solar assisted main parameters

The main parameters	Coal-fired units	Coal-carbon capture unit	Solar assisted coal - carbon capture scheme I
Unit output power MW	1074.47	854.44	1091.889
Circulating thermal efficiency %	51.17	44.06	53.65
Standard coal consumption rate g/(kW · h)	268.5	315.67	259.22
Heat consumption rate kJ/(kW · h)	7292.12	8340.1	6848.49
Secondary reheat flow kg/s	594.11	230.77	391.543
CO <sub>2</sub> emission rate g/(kW · h)	700.65	122.06	100.23

Can be concluded from table 5.3, as coal-fired units have been added for carbon capture unit energy consumption caused by the reboiler is required by the high pressure cylinder exhaust steam of the steam into the second reheat extraction steam, making into the second reheat steam flow rate decreased by 363.34 kg/s, due to a large number of steam is used to provide carbon capture the consumption of reboiler, making coal - carbon capture unit of output than the original dropped by 220.03 MW coal-fired unit, circulation has fallen by 7.11%, thermal efficiency energy huge punishment. On the basis of the coal-carbon capture system, the unit output increased by 237.449MW, the circulating thermal efficiency increased by 9.59 percentage points, and the CO<sub>2</sub> emission rate decreased by 21.83g/(kWh). For 1000MW coal-fired units, after the introduction of solar energy, the unit output increased by 17.42MW, the coal consumption decreased by 9.28g/(kWh), the CO<sub>2</sub> emission rate decreased by 594.87g/(kWh), and the decarbonization rate reached 85%.

**5.3 Exergy analysis**

Exergy is defined as that when a system changes reversibly from any state to another equilibrium state, a part of the energy can be transformed into other energies indefinitely. This part of the energy is the available energy and is called exergy. The thermal analysis method based on the first law of thermodynamics can be used for quantitative analysis of thermal economy. And based on the second law of thermodynamics exergic analysis [60], can be used for qualitative analysis of the thermal efficiency of the system, and the rationality of the evaluation system of energy utilization, find out the energy using the best equipment, larger energy loss and mining equipment, analyzes the cause of the loss and puts forward improving plan, in order to achieve the purpose of comprehensive energy saving. Exergic efficiency refers to the effective utilization degree of the system for exergy input, that is, the ratio of exergy generating effective utilization value to net exergy input [58]. Through exergic efficiency calculation, the effect of energy conversion and the degree of effective utilization can be determined, and the rationality of energy distribution of the system can be analyzed. In all irreversible processes, there is the devaluation of energy, and some useful energy will degenerate into useless energy, resulting in exergy loss.

**5.3.1 Exergic analysis model for each equipment**

(1) boiler

					<i>13.04.01.2020.286.YY EN</i>	<i>page</i>
						55
<i>ИЗМ</i>	<i>Page</i>	<i>Document #</i>	<i>Signat.</i>	<i>Date</i>		

In a boiler, the heat released by burning coal is transferred to the feed water through the boiler and becomes superheated steam. A exergy that burns coal is a exergy that is put into the boiler as a exergy, while a exergy that generates effective use value is a exergy that is the exergy of main steam and reheat steam.

Exergy loss of boiler can be calculated as follows:

$$I_b = Be_f - D_0(e_0 - e_{fw}) - D_{rh1}(e_{rh1}^{out} - e_{rh1}^{in}) - D_{rh2}(e_{rh2}^{out} - e_{rh2}^{in}) \quad (5.1)$$

The calculation formula of exergic efficiency of boiler is as follows:

$$\eta_b = \frac{D_0(e_0 - e_{fw}) + D_{rh1}(e_{rh1}^{out} - e_{rh1}^{in}) + D_{rh2}(e_{rh2}^{out} - e_{rh2}^{in})}{Be_f} \quad (5.2)$$

Where:

$I_b$  —Exergy loss of boiler, kW;

$B$  —Coal consumption of coal-fired units,kg/s;

$e_f$  —Coal burning chemical exergy,kJ/kg;

$D_0$  —Main steam flow, kg/s;

$e_0$  ,  $e_{fw}$  —Ratio exergy of main steam, ratio exergy of water supply, kJ/kg;

$D_{rh1}$  —Flow rate of primary reheat steam, kg/s;

$e_{rh1}^{in}$  ,  $e_{rh1}^{out}$  —Ratio exergy of reheat steam inlet and outlet,kJ/kg;

$D_{rh2}$  —Flow rate of secondary reheat steam,kg/s;

$e_{rh2}^{in}$  ,  $e_{rh2}^{out}$  —Ratio exergy of secondary reheat steam inlet and outlet,kJ/kg;

Exergy of coal can be calculated as follows:

$$e_f = Q_{net,ar} (1.0064 + 0.1519 \frac{\omega(H)}{\omega(C)} + 0.616 \frac{\omega(O)}{\omega(C)} + 0.0429 \frac{\omega(N)}{\omega(C)}) \quad (5.3)$$

Where:

$\omega(C)$  ,  $\omega(H)$  ,  $\omega(O)$  ,  $\omega(N)$  —the mass fraction of carbon, hydrogen, oxygen and nitrogen of coal, %.

					13.04.01.2020.286.YY EN	page
						56
ИЗМ	Page	Document #	Signat.	Date		

## (2) Turbines

In turbine, spinning into the superheated steam of the turbine to drive the impeller impeller of superheated steam heat energy can be converted to mechanical energy, in this process, the superheated steam Exergy value minus the exhaust steam Exergy and extraction steam Exergy value after got is into the net Exergy of steam turbine, and the effective utilization of value is generated by the impeller rotating shaft work. Therefore, exergy loss of steam turbine can be calculated as follows:

$$I_t = D_{nt}^{in} e_{nt}^{in} - D_{nt}^{out} e_{nt}^{out} - D_{nt}^{ex} e_{nt}^{ex} - W_{nt} \quad (5.4)$$

Exergic efficiency of steam turbine can be calculated as follows:

$$\eta_t = \frac{W_{nt}}{D_{nt}^{in} e_{nt}^{in} - D_{nt}^{out} e_{nt}^{out} - D_{nt}^{ex} e_{nt}^{ex}} \quad (5.5)$$

Where:

$I_t$ —Exergy of turbine, kW;

$\eta_t$ —Exergic efficiency of steam turbine, %;

$D_{nt}^{in}$  ,  $e_{nt}^{in}$  — The flow and exergy of steam entering the turbine at the n-th stage,kg/s; kJ/kg;

$D_{nt}^{out}$  ,  $e_{nt}^{out}$  — The flow and exergy of steam exiting the turbine at the n-th stage,kg/s; kJ/kg;

$D_{nt}^{ex}$  ,  $e_{nt}^{ex}$  —The flow and exergy of extracts steam at the n-th stage,kg/s; kJ/kg;

$W_{nt}$ —The output shaft work of the n-th turbine,kW.

## (3) regenerative heater

Heat recovery heater mainly USES steam extraction from steam turbine to heat feed water and condensate water, so as to improve the efficiency of Rankine cycle. Therefore, for the return heat heater, exergy of steam extraction and exergy of the superior return heat heater minus exergy of the corresponding level are worth to be the net exergy of the current level heater, while exergy of effective utilization is exergy generated after heating the water supply and condensate.

Exergy loss of regenerative heater can be calculated as follows:

					<i>13.04.01.2020.286.YY EN</i>	<i>page</i>
						57
<i>ИЗМ</i>	<i>Page</i>	<i>Document #</i>	<i>Signat.</i>	<i>Date</i>		

$$I_n = D_i e_i + D_{dw(i-1)} e_{dw(i-1)} - D_{dw(i)} e_{dw(i)} - D_i^{in} (e_i^{out} - e_i^{in}) \quad (5.6)$$

Exergic efficiency of regenerative heater:

$$\eta_n = \frac{D_i^{in} (e_i^{out} - e_i^{in})}{D_i e_i + D_{dw(i-1)} e_{dw(i-1)} - D_{dw(i)} e_{dw(i)}} \quad (5.7)$$

Where:

$I_n$  — Exergy loss of regenerative heater, kW;

$\eta_n$  — Exergic efficiency of regenerative heater, %;

$D_i$  ,  $e_i$  — The exhaust flow and exergy ratio of the level-i regenerative heater, kg/s; kJ/kg;

$D_{dw(i-1)}$  ,  $e_{dw(i-1)}$  — The hydrophobic flow rate and exergy ratio of the level-i-1 regenerative heater , kg/s; kJ/kg;

$D_{dw(i)}$  ,  $e_{dw(i)}$  — The hydrophobic flow rate and exergy ratio of the level-i regenerative heater , kg/s; kJ/kg;

$D_i^{in}$  — Feed water flow at the inlet of the level-i regenerative heater, kg/s;

$e_i^{in}$  ,  $e_i^{out}$  — The inlet and outlet exergy ratio of the level-i regenerative heater, kg/s; kJ/kg.

#### (4) pump

The pump is the pressurization equipment of the system. For the pump, exergy that can be effectively used is the increase of exergy that can be pumped, while exergy that can be put into the system is the work consumed by the pump.

Exergic efficiency of the pump can be calculated as follows:

$$\eta_p = \frac{D_p (e_p^{out} - e_p^{in})}{W_p} \quad (5.8)$$

The calculation formula of exergy of the pump is as follows:

$$I_p = W_p - D_p (e_p^{out} - e_p^{in}) \quad (5.9)$$

					<i>13.04.01.2020.286.YY EN</i>	<i>page</i>
						58
<i>ИЗМ</i>	<i>Page</i>	<i>Document #</i>	<i>Signat.</i>	<i>Date</i>		

Where:

$\eta_p$  —Exergic efficiency of pump, %;

$D_p$  —Flow rate into the pump, kg/s;

$e_p^{\text{in}}$  —The inlet flow exergy ratio of the pump, kJ/kg;

$e_p^{\text{out}}$  —The outlet flow exergy ratio of the pump, kJ/kg;

$W_p$  —Work consumed in the pump, kW.

### (5) carbon capture system

Adding carbon capture system to capture the carbon dioxide from the burning of coal-fired units, capture requires a lot of energy, in the scheme I and II , this part of the energy provided by the coal-fired units turbine extraction, in the scheme III provided by the solar field. So for carbon capture system, the net exergy input system of scheme II and I is the steam entering the carbon capture system to do work and the exergy of cooled water minus the outlet water exergy values of carbon capture system. The net exergy input system of scheme III is solar field exergy export steam and the exergy of cooled water minus the export water exergy values of carbon capture system, effective value is the energy consumed in the reboiler.

The calculation formula for exergy of the carbon capture system is as follows:

$$I_c = D_c^{\text{in}} e_c^{\text{in}} + D_c^{\text{de}} e_c^{\text{de}} - D_c^{\text{out}} e_c^{\text{out}} - W_c \quad (5.10)$$

Exergic efficiency of the carbon capture system can be calculated as follows:

$$\eta_c = \frac{W_c}{D_c^{\text{in}} e_c^{\text{in}} + D_c^{\text{de}} e_c^{\text{de}} - D_c^{\text{out}} e_c^{\text{out}}} \quad (5.11)$$

Where:

$I_c$  —Exergy loss of carbon capture system, kW;

$\eta_c$  —Exergic efficiency of carbon capture system, %;

$D_c^{\text{in}}$  ,  $e_c^{\text{in}}$  — Steam flow rate and exergy ratio into the carbon capture system, kg/s;kJ/kg

$D_c^{\text{de}}$  ,  $e_c^{\text{de}}$  —Steam flow rate and exergy ratio of spraying water kg/s;kJ/kg;

					13.04.01.2020.286.YY EN	page
						59
ИЗМ	Page	Document #	Signat.	Date		



$D_c^{\text{out}}$  ,  $e_c^{\text{out}}$  — Steam flow rate and exergy ratio of carbon capture system exports water kg/s; kJ/kg;

$W_c$ —Work consumed in the reboiler, kW.

### (6) Solar thermal field

Solar energy collecting field using solar radiant energy to heat supply water instead of high pressure regenerative heater, low pressure regenerative heater and supply energy to carbon capture system. For a solar collector field, the input is the solar radiant energy absorbed by the solar collector field, while effective utilization is the exergy resulting from the supply water heated by the solar collector field.

Therefore, the exergy of a solar field:

$$I_{\text{solar}} = Q_{\text{solar}} - D_{\text{solar}}^{\text{in}} (e_{\text{solar}}^{\text{out}} - e_{\text{solar}}^{\text{in}}) \quad (5.12)$$

Exergic efficiency of solar thermal field:

$$\eta_{\text{solar}} = \frac{D_{\text{solar}}^{\text{in}} (e_{\text{solar}}^{\text{out}} - e_{\text{solar}}^{\text{in}})}{Q_{\text{solar}}} \quad (5.13)$$

Where:

$I_{\text{solar}}$  —Exergy loss of solar field, kW;

$\eta_{\text{solar}}$  —Exergic efficiency of solar field, %;

$Q_{\text{solar}}$  —Solar radiant energy absorbed by solar thermal field, kW;

$D_{\text{solar}}^{\text{in}}$  —Supply water flow into the solar heat collection field, kg/s;

$e_{\text{solar}}^{\text{in}}$  ,  $e_{\text{solar}}^{\text{out}}$  — The exergy ratio of the supply water at inlet and outlet of solar thermal field kg/s,kJ/kg.

### 5.3.2 Exergic calculation results

Set based on the above theory, the environment temperature is 20 °C , pressure is 0.1 MPa, for reference of scheme C, and I , scheme II , scheme III ,calculating the exergy loss and exergy efficiency, find which scheme is the best,at the meanwhile analysis the reason to improve.

					<i>13.04.01.2020.286.YY EN</i>	<i>page</i>
						60
<i>ИЗМ</i>	<i>Page</i>	<i>Document #</i>	<i>Signat.</i>	<i>Date</i>		

Exergy balance calculation of coal-fired units can be simulated by EBSILON software. Exergy analysis of the thermal side of boiler, turbine and reheat system is carried out in this chapter. According to the location of the extraction point, the steam turbine is divided into 11 stages, among which the ultra-high pressure cylinder is the first stage, the high-pressure cylinder is the second stage, the medium-pressure cylinder is the third stage, the low-pressure cylinder is the fifth stage, and the reheater is the ninth stage. The results are calculated and obtained respectively.

Exergic calculation results of each scheme are shown in the following table.

Table 5.4 Exergic calculation results

Equipment	Scheme C		Scheme I		Scheme II		Scheme III	
	Exergic loss MW	Exergic efficiency %	Exergic lossMW	Exergic efficiency cy%	Exergic lossMW	Exergic efficiency ncy%	Exergic loss MW	Exergic efficiency %
Boiler	757.42	56.61	922.84	56.81	759.2	56.62	797.22	56.78
Ultra-high pressure cylinder	10.48	95.45	10.48	95.45	10.48	95.45	10.48	95.45
High pressure cylinder # 1	3.48	97.12	3.9	97.12	3.48	97.12	3.48	97.12
High pressure cylinder # 2	3.9	96.71	4.73	96.71	3.9	96.71	3.9	96.71
Medium pressure cylinder # 1	0.7	97.6	1.19	97.6	0.74	97.6	1.54	97.6
Medium pressure cylinder # 2	1.87	97.15	3.17	97.15	1.97	97.15	4.1	97.15
Medium pressure cylinder # 3	1.13	96.82	1.91	96.82	1.19	96.82	2.47	96.82
Low pressure cylinder # 1	0.25	95.38	0.47	95.38	0.27	95.38	0.63	95.38
Low pressure cylinder # 2	2.01	94.5	3.78	94.5	2.13	94.5	5.07	94.5
Low pressure	2.35	93.24	4.44	93.24	2.87	93.24	5.97	93.24

cylinder # 3								
Low pressure cylinder # 4	2.41	91.92	4.57	91.92	2.87	91.92	6.16	91.92
Low pressure cylinder # 5	4.98	82.04	9.48	82.04	6.22	82.04	12.8	82.04
High pressure reheater # 1								
High pressure reheater # 2	5.52	92.57	0.0	92.57	5.52	92.57	5.52	92.57
High pressure reheater # 3	3.15	93.86	0.0	93.86	3.15	93.86	3.15	93.86
High pressure reheater # 4	1.59	95.1	0.0	93.25	2.17	93.25	1.59	95.1
Low pressure reheater # 5	0.22	96.43	0.15	97.13	0.0	95.69	0.38	95.7
Low pressure reheater # 6	0.34	93.67	0.58	93.62	0.0	93.63	0.75	93.64
Low pressure reheater # 7	1.14	86.84	1.96	86.7	0.0	86.74	2.54	86.74
Low pressure reheater # 8	0.97	84.91	1.66	84.77	0.0	84.81	2.15	84.81
Low pressure reheater # 9	0.74	80.66	1.27	80.51	0.0	80.55	1.64	80.55
Feed pump system	7981	78.76	8247	78.76	8247	78.76	7981.26	78.76
Deaerator	1549	98.69	2118.89	98.22	1797	98.49	1549.76	98.69
Carbon capture turbine # 1								
Carbon capture turbine # 2	3.08	95.13	3.14	95.13	2.97	95.13	0.68	95.13
Carbon capture turbine # 3	2.79	94.46	3.07	94.46	2.69	94.46	0.45	94.46
Carbon capture turbine # 4	2.63	93.68	2.8	93.68	2.51	93.68	0.24	93.68
Carbon capture	2.4	86.27	2.57	86.27	2.35	86.27	0.13	86.27

turbine # 5								
Condenser system	13120	74.72	22170	74.67	16200	74.06	28586	74.69
Carbon capture system	24.54	88.12	25.01	88.24	23.98	88.24	25.34	88.22
Solar energy field	—	—	287.25	49.45	78.99	23.81	479.24	30.95
Total exergy loss	23494	—	33836	—	27168	—	39498	—

As can be seen from table 5.4, exergy of the boiler suffered the greatest loss while exergy efficiency was the lowest, so exergy had a great energy saving potential. Exergy efficiency of coal-fired boiler is mainly caused by exergy irreversible loss in the combustion process and exergy irreversible loss in the heat transfer process. Due to the difference in the level of the chemical energy of fuel and combustion products, produces in the process of energy conversion part exergy loss, this part exergy loss is not reversible, but can improve the combustion environment to reduce this part exergy losses, make this difference control in a reasonable range: use the design of coal; under the condition of ensuring the full combustion of fuel, the air supply should be reduced in an appropriate amount to reduce the furnace leakage, reduce the excess air coefficient, and reduce the loss of smoke emission and heat dissipation through reasonable air distribution [59].

Before the superheated steam enters the turbine, it has to pass through the main steam valve, regulating valve, steam chamber, pipeline and other equipment. It will inevitably cause throttling loss, which is irreversible loss. As can be seen from table 5.4, exergic loss ratio of steam turbine is much lower than that of boiler. Exergic efficiency of the first stage medium pressure cylinder of steam turbine is the highest, and exergic efficiency is the highest in the whole coal burning system. The working medium in this process is superheated steam, with high thermodynamic efficiency. Exergy is the largest in the last stage of the low-pressure cylinder of steam turbine. The last stage of the low-pressure cylinder is in the state of wet steam, resulting in a large loss of wet steam. Therefore, the energy saving optimization of the turbine should focus on the optimization of the low-pressure cylinder of steam turbine. Exergic efficiency of the high-pressure reheater in the three schemes is basically lower than scheme C. From the perspective of exergic efficiency of the reheating heater at all levels, exergic efficiency of the reheating heater continues to decline with the reduction of the quality of the steam extraction, especially in the last two stages.

Solar thermal field's exergic efficiency is the lowest of the whole solar assisted coal-fired units carbon capture system, except for the optical properties of collector and medium heat absorption in the absorber, and sets of thermal field for a wide variety of line loss, the pipe is high temperature heat conduction oil, heat loss is larger. Therefore, in addition to improving the optical properties of the collector, the optimization of the side of the solar heat collection field should also reasonably plan the pipeline layout of the solar heat collection field to reduce the loss in the pipeline. At the same time, pay attention to the use of insulation equipment to reduce the heat dissipation of the pipeline in the heat collection field.

The total exergic loss of scheme I greater than scheme II less than scheme III, after analysis found that for scheme I ,due to the solar field replaced the high-pressure reheater, made of high quality high pressure extraction to continue to work in steam turbine, enhancing the thermal efficiency of the unit, also made the reheat steam flow into the boiler is bigger than the rest of the several schemes is that can make boiler exergic loss is larger. Solar field replaced high-pressure reheater, no high temperature hydrophobic into the deaerator, but the feed water flow into the deaerator is greater than other schemes, so for scheme I ,deaerator exergic loss also larger. It can also be seen from table 5.4 that after replacing the high-pressure regenerative heater with a solar thermal field, exergy loss is zero without high steam pumping. Scheme II is solar field instead of the low pressure reheater, high pressure of the reheater exergic loss increased significantly, and low pressure reheater exergic loss is zero.

The parameters of the three schemes are the same except the inlet and outlet temperature and the working medium flow into the solar energy collecting field. The carbon capture system and the solar field exergic loss of scheme II is lower than scheme I and III, because that, the fluid temperature and flow rate into the solar thermal field of scheme II are smaller than those of scheme I and III. By the same token, the fluid temperature and flow rate into the solar thermal field of scheme I are higher than the rest of the two kinds of schemes, so the exergic loss is higher, at the same time, the exergic efficiency is higher, the effect of the conversion of solar energy is reasonable.

#### 5.4 Economic comparison

The investment of solar thermal field is \$257 /m<sup>2</sup>. The area of solar thermal field can be calculated by thermal balance. In this paper, the exchange rate between us dollar and RMB is 7. Power plant construction and additional costs account for 20%, operation and maintenance costs are 3%, equipment service life is 30 years, the average solar

					<i>13.04.01.2020.286.YY EN</i>	<i>page</i>
						64
<i>ИЗМ</i>	<i>Page</i>	<i>Document #</i>	<i>Signat.</i>	<i>Date</i>		

power operating hours are 1469h per year at full load. Table 5-5 shows the economic parameters of the solar thermal field of the three schemes.

Table 5.5 economic parameters of solar thermal field of three schemes

Project	Scheme I	Scheme II	Scheme III
Coal consumption with solar energy g/(kW · h)	259.22	310.32	273.57
Coal consumption without solar energy g/(kW · h)	315.67	315.67	315.67
Total system output power /MW	1092	871	1041
Collector field power /MW	492.83	95.58	650.52
Collector field area /km <sup>2</sup>	1.12	0.22	1.50
Catching carbon/(t/h)	620.15	592.52	624.77
Solar energy annual carbon capture /t	911000.35	870411.88	917787.13
Collector area required per unit CO <sub>2</sub> (m <sup>2</sup> /t)	1.23	0.25	1.63
Total investment cost of collector /M\$	288.82	55.54	384.74
Power plant construction and additional cost /M\$	57.76	11.11	76.95
Annual operation and maintenance cost /M\$	8.66	1.67	11.54
Average annual investment coefficient of equipment	0.09	0.09	0.09
Equipment annual investment cost /M\$	31.19	6.00	41.55

Table 5.6 Power plant cost data [41,56]

Parameter	Value
Initial construction of coal-fired power plant /M\$	507.14
Desulfurization equipment /M\$	45.00
Denitration equipment /M\$	40.36
Decarbonizing equipment /M\$	230.10
Decarburization turbine /M\$	2.86
Annual operation and maintenance cost /M\$	33.02
MEA cost (\$/tCO <sub>2</sub> )	0.24

Coal price (\$/t)	134.29
Running hours /h	5000

The results are reflected in table 5.7.

Table 5.7 comparison of economic evaluation of integrated system

Indicators	Coal-fired units	Scheme	Scheme	Scheme	Scheme
		C	I	II	III
Coal saving ratio for investment	—	—	0.028	0.014	0.016
Average solar cost of carbon capture (\$/t)	—	—	43.75	8.81	57.85
Levelized Cost of Energy (\$/MW·h)	47.64	240.75	66.30	63.75	67.74

Coal saving ratio for investment can reflect payback period of solar thermal field, The greater coal saving ratio, the shorter payback period [50]. Can be seen from table 5.7, coal saving ratio for investment: the scheme I > scheme III > scheme II, get that scheme I is the shortest investment recovery period, the longest period is the scheme II.

Comparing three kinds of schemes and the original coal-fired power plants and after cost calculation about the life cycle of coal-fired power plants based on carbon capture, found that pure coal-fired power generating cost is 47.64 (\$/MW·h), after adding carbon capture unit, power generation cost is 240.75 (\$/MW·h), cost increased by 193.11 (\$/MW·h). It can be seen that the carbon capture coal-fired units without external auxiliary energy are less economical. The cost of power generation of the three schemes using solar energy is lower than that of scheme C, which is about 30% of that of scheme C.

Average solar cost of carbon capture: scheme II < scheme I < scheme III, because solar energy utilization on scheme II is the least, so the average cost of solar is the lowest. However, the more solar energy is utilized within a certain investment cost range, the better it will be for the targets of the realization of energy conservation and emission reduction. While the levelized cost scheme I is higher than scheme II, but for the

scheme I coal saving ratio for investment is higher than the scheme II , investment recovery period is short.And through the analysis of the thermal performance in the previous section known the coal consumption of scheme II is higher than scheme I about 51.1 g/(kWh), CO<sub>2</sub> emissions higher than scheme I about 19.76 g/(kWh),cycle thermal efficiency is 8.84% lower than the scheme I , thermodynamic performance is poorer, scheme II is the unreasonable scheme for solar assisted coal carbon capture. The coal consumption of scheme I are lower than scheme III about 14.35 g/(kWh), CO<sub>2</sub> emission rates lower than scheme III about 5.55 g/(kWh), at the same time,thermal efficiency higher 2.82% , the thermal performance is better than the schemeIII, and the electricity cost and average solar energy costs of scheme I are lower than schemeIII, Coal saving ratio for investment is higher than scheme III , considering thermal performance and economic performance scheme I are optimal.

#### SUMMARY AND PROSPECT

Since the additional carbon capture system consumes a large amount of energy, the output of the original coal-fired units is greatly reduced. Therefore, the solar thermal field is introduced in this chapter as an external energy source to compensate for the energy penalty caused by the carbon capture system. Consider three kinds of method of integration: solar energy and the high pressure reheat systems integration (scheme I ); Solar energy system with low pressure reheat systems integration (scheme II ); Solar energy system and carbon capture system integration (scheme III), coal - carbon capture simulate the optimal scheme for the object system, implements three integration modeling. Based on the optimal scheme simulated by the coal-carbon capture system, three integrated schemes are modeled. Compared with thermal performance and economic performance, three schemes of carbon capture in solar-assisted coal-fired power plants were analyzed, exergy loss and exergic efficiency calculation models of all equipment were analyzed, exergy loss and exergic efficiency calculation of the reference unit and three schemes were performed, respectively. The following conclusions were drawn through the display of the results and chart analysis:

Simulated solar assisted coal - carbon capture system, the schema I solar energy regenerative system instead of high pressure , the cycle thermal efficiency is the highest, the CO<sub>2</sub> emission rate and coal consumption rate is the lowest. When solar energy was introduced to replace the high pressure reheater, the units output increased by 17.42MW,

					<i>13.04.01.2020.286.YY EN</i>	<i>page</i>
						67
<i>ИЗМ</i>	<i>Page</i>	<i>Document #</i>	<i>Signat.</i>	<i>Date</i>		



the coal consumption decreased by 9.28g/(kWh), the CO<sub>2</sub> emission rate decreased by 594.87g/(kWh), and the decarbonization rate reached 85%. At the same time, solar photoelectric conversion efficiency of scheme I is higher than III and II, is the best solution for solar energy conversion degree.

Although the average cost of solar of scheme II is the lowest, solar energy utilization on scheme II is the least, coal saving ratio for investment is less than the scheme I, investment recovery period is long. And the thermal performance is the worst, practical for solar investment a waste. The power generation cost of scheme I is higher than scheme III about 0.95( \$/MW·h ), but the coal saving ratio of scheme I is higher than the scheme III, investment recovery period is short, at the same time, average solar energy cost of carbon capture is less than the scheme III, and by 5.2.1 section of thermal performance analysis shows that coal consumption of scheme I are lower than scheme III about 14.35 g/(kWh), CO<sub>2</sub> emission rates low about 5.55 g/(kWh), at the same time, thermal efficiency high 2.82%, thermal performance is superior to the scheme III.

Exergy loss of boiler accounted for more than 90% of overall exergy loss, and exergic efficiency was the lowest, so exergy had great energy saving potential. Steam turbine is the part that does the most work in the whole unit, and exergic efficiency is the highest. Among them, because of the wet steam loss of the low-pressure cylinder, exergy loss of the low-pressure cylinder is the largest in the steam turbine system, and exergic efficiency is also the lowest in the steam turbine system. After the carbon capture of the coal-fired units assisted by solar energy, exergy efficiency of the solar energy collecting field is the lowest, while exergy loss is the largest except boiler. In addition to exergy loss caused by the entropy increase of medium heat absorption and temperature rise in the absorber, there are also pipeline loss and heat dissipation loss of heat-conducting oil. The solar energy collector field efficiency of scheme I is higher than that of scheme II and scheme III, and the effective utilization rate of solar energy is the highest. The solar energy collector field in Scheme II has the lowest efficiency and the solar energy utilization is extremely unreasonable. At the same time, the loss of solar energy collector field of scheme I is less than that of scheme III, and the irreversible loss is small, so scheme I is considered to be the most reasonable scheme for solar energy utilization.

					<i>13.04.01.2020.286.YY EN</i>	<i>page</i>
						68
<i>ИЗМ</i>	<i>Page</i>	<i>Document #</i>	<i>Signat.</i>	<i>Date</i>		

## SUMMARY AND PROSPECT

Based on the principles of environmental protection, this paper analyzes the carbon capture technology of 1000MW coal-fired power plants for the purpose of reducing carbon emissions from coal-fired power plants. Provide six different steam supply schemes for carbon capture of 1000MW secondary reheat coal-fired power plants, respectively scheme A for taking steam from primary reheating cold section, scheme B for taking steam from primary reheating hot section, secondary reheating Scheme C for taking steam in the cold section, Scheme D for taking steam in the secondary reheating hot section, Scheme E for taking steam at the connection of the medium and low pressure cylinders, and comparison of the medium and low pressure cylinders with the addition of a small back pressure machine at the connection of the medium and low pressure cylinders Scheme F with no small back pressure at the connection. Relying on EBSILON thermal balance simulation software to simulate and calculate six different schemes, the scheme with the least disturbance to the coal-fired unit and the best performance parameters is selected by comparing the performance indexes of the different schemes. The addition of a carbon capture unit will cause huge energy penalties for the operation of the original coal-fired unit. Based on this, this paper proposes a complementary energy utilization method of solar-assisted coal-fired power plants for carbon capture. Three integration methods are proposed, scheme I of solar energy and high-pressure recuperation system integration, scheme II of solar energy and low-pressure recuperation system integration, and scheme III of solar energy and carbon capture system integration. The three integrated methods were used to evaluate the thermal performance such as CO<sub>2</sub> emission rate, coal consumption rate, unit thermal cycle efficiency and solar photovoltaic conversion efficiency. It also introduces economic indicators such as investment in coal-saving ratio, average solar carbon capture cost and levelized power generation cost to evaluate the economics of different integration schemes. In order to evaluate the rationality of the system's energy utilization, this paper uses the exergy balance analysis method based on the second law of thermodynamics to analyze the exergy loss and exergy efficiency of the three integrated schemes of complementary light coal. Concluded as follow:

(1) After adding a carbon capture device to the coal-fired system, the energy penalty is huge, the total power of the system drops by 220.03MW, and the cycle thermal efficiency drops by 7.11 percentage points. 363.34 kg / s was extracted from the steam extracted from the high-pressure cylinder, and nearly 60% of the steam was used to provide the regeneration energy consumption of the reboiler of the carbon capture unit. Among the six coal-carbon capture and steam supply schemes, scheme C, when

					<i>13.04.01.2020.286.YY EN</i>	<i>page</i>
						69
<i>ИЗМ</i>	<i>Page</i>	<i>Document #</i>	<i>Signat.</i>	<i>Date</i>		

the steam is supplied from the secondary reheat cooling section, the unit's circulating thermal efficiency is the highest, 44.06%, and the CO<sub>2</sub> emission rate is the lowest, as low as 122.06g / kWh), the standard coal consumption rate and heat consumption rate of power generation are the lowest, which is the best solution.

(2) In the scheme study of carbon capture for solar-assisted coal-fired units, compared with scheme II, scheme I has a coal consumption of 51.1g/(kW·h) lower than scheme II, and CO<sub>2</sub> emissions are 19.76g/(kW·h) lower than scheme II. The cycle thermal efficiency is 8.84 percentage points higher than that of Scheme II; compared with Scheme III, the coal consumption is 14.35g/(kW·h) lower, the CO<sub>2</sub> emission rate is 5.55g/(kW·h) lower, and the thermal efficiency is 2.82 percentage points higher, which is the the best solution in thermal performance of the three schemes. At the same time, the solar photovoltaic conversion efficiency of scheme I is higher than that of scheme II and scheme III, which is the best scheme for solar energy conversion. After the introduction of solar heat, the circulating thermal efficiency of the unit is significantly higher than that without the introduction of solar energy, and the standard coal consumption rate and CO<sub>2</sub> emission rate of power generation are significantly lower than those without the introduction of solar energy.

(3) The efficiency of the solar heat collecting field of scheme I is higher than that of scheme II and scheme III, and the effective utilization rate of solar energy is the highest. Scheme II has the lowest efficiency and the solar energy utilization is extremely unreasonable. The energy loss of the solar heat collecting field of scheme I is less than that of scheme III, and the irreversible losses are small.

(4) After the addition of a carbon capture unit, the cost of power generation is 240.75( \$/MW·h ), which is an increase of 193.11( \$/MW·h ) compared to the original coal-fired unit. The cost of power generation using the three solar-assisted schemes is lower than that of scheme C, which is 30% of Option C, it can be seen that although the initial investment of the solar thermal field of the carbon capture system of the solar-assisted coal-fired power plant is relatively large, the power generation cost within the operating life of the unit is lower than that of the pure coal-carbon capture unit.

(5) According to the economic analysis results of the three integration schemes, the investment coal saving ratio of scheme I is greater than that of scheme II and scheme III, and the investment recovery period is short; meanwhile, the average cost of solar carbon capture is less than that of scheme III, and when scheme I is adopted The efficiency of the solar thermal field is higher than the other two schemes, and the utilization of solar

					<i>13.04.01.2020.286.YY EN</i>	<i>page</i>
						70
<i>ИЗМ</i>	<i>Page</i>	<i>Document #</i>	<i>Signat.</i>	<i>Date</i>		

energy is the most reasonable. The levelized power generation cost of scheme I is 41.44 ( \$/MW·h ), which is 0.74 ( \$/MW·h ) lower than scheme II , and 0.95 ( \$/MW·h ) higher than scheme III . It is not the most economical solution in terms of power generation cost. However, after adopting scheme I , the output of coal-fired power plant units increased by 17.42MW, coal consumption was reduced by 9.28g / (kWh), the CO<sub>2</sub> emission rate was reduced by 594.87g / (kWh), and the decarbonization rate reached 85%, which is the maximum. The use of solar energy has effectively reduced carbon dioxide emissions. If relevant policies can be adopted to increase government subsidy support and reduce pre-construction costs, then solar-assisted coal-carbon capture technology will be an effective measure to achieve the major goal of energy conservation and emission reduction.

### Outlook

China's research on carbon capture in solar-assisted coal-fired power plants is not comprehensive enough, and there is still a large research space. The follow-up research work can be started from the following aspects:

(1) This article only analyzes the design conditions of the unit, and does not consider the operation of variable conditions. In actual operation, the load of the unit changes with the dispatch of the power grid at any time, and the performance of each parameter of the unit will also deviate from the design parameters, so the analysis of the unit's variable operating conditions is also an important follow-up work in this research direction.

(2) The calculation of the economics of the integrated system does not consider the recovery and sale of CO<sub>2</sub>. Subsequent research can analyze the use value of CO<sub>2</sub> from the perspective of economics to make up for the cost of the integrated system to a certain extent.

(3) The research in this article is only at the level of theoretical analysis and simulation calculation. Experimental research can be carried out in the future, and the theoretical calculation can be verified with experimental data.

### REFERENCES

					<i>13.04.01.2020.286.YY EN</i>	<i>page</i>
						71
<i>ИЗМ</i>	<i>Page</i>	<i>Document #</i>	<i>Signat.</i>	<i>Date</i>		

1 Ding Yihui, Zhang Jin. Changes in extreme weather and climate events and their relationship with global warming — commemorating the 2002 World Meteorological Day "Reducing vulnerability to extreme weather and climate events" [J]. Meteorology, 2002, 3: 3-7.

2 IPCC. 2006 IPCC guidelines for national greenhouse gas inventories[R]. Kanagawa, Japan: IPCC National Greenhouse Gas Inventory Program, 2006.

3 IPCC. Special report on emissions scenarios: a special report of working group III of the Intergovernmental Panel on Climate Change,92-9169-1135, Cambridge University Press, New York (2000).

4 IEA. Energy Technology Perspectives 2008: Scenarios and strategies to 2050[R]. IEA, Paris, France: IEA/OECD, 2008.

5 Xu Youbo, Zhao Ming, Qiu Yalin, Zhou Chi, Gu Pengfei, Xiang Wenguo. Solar CaO high-temperature heat storage assisted CO<sub>2</sub> capture coal-fired power generation system [J]. Journal of Solar Energy, 2017,38 (01): 180-185.

6 Jamel M. S., Abd Rahman A., Shamsuddin A. H. Advances in the integration of solar thermal energy with conventional and non-conventional power plants[J]. Renewable and Sustainable Energy Reviews, 2013,20:71-81

7 Peterseim J. H., White S., Tadros A., et al. Concentrated solar power hybrid plants, which technologies are best suited for hybridisation?[J]. Renewable Energy, 2013,57:520-532.

8 Sun Xiqiang, Yi Changtao. Northwest Coal Power Base implements the light coal complementary concept [N]. China Electric Power News, 2016-01-23.

9 Liu Dan. Jin Hongguang: Should vigorously develop medium and low temperature solar power generation technology [J]. SME Management and Technology (Mid-Term), 2010 (05): 70-71.

10 IEA.Towards Zero Emission Coal-fired Power Plants Clean Coal Centre,Report CCC/101,2005.

11 International Energy Agency. World Energy Outlook 2015 [M]. Beijing: China Petrochemical Press, 2016.

					<i>13.04.01.2020.286.YY EN</i>	<i>page</i>
						72
<i>ИЗМ</i>	<i>Page</i>	<i>Document #</i>	<i>Signat.</i>	<i>Date</i>		

12 R.J. Zoschak, S.F. Wu, Studies of the direct input of solar energy to a fossil-fueled central station steam power plant, Solar Energy, Volume 17, Issue 5, 1975, Pages 297-305, ISSN 0038-092X

13 YANG Y, HU E J. Thermodynamic advantages of using solar energy in the regenerative Rankine power plant[J]. Applied Thermal Engineering, 1999, 19(11): 1173–1180.

14 Eric Hu, YongPing Yang, Akira Nishimura, Ferdi Yilmaz, Abbas Kouzani, Solar thermal aided power generation, Applied Energy, Volume 87, Issue 9, 2010, Pages 2881-2885, ISSN 0306-261

15 Q. Yan, E. Hu, Y. Yang, et al. Evaluation of solar aided thermal power generation with various power plants[J]. International Journal of Energy Research, 2011, 35(10): 909-922

16 Reddy, V. Siva, Kaushik, S. C, Tyagi, S. K. Exergetic analysis of solar concentrator aided coal fired super critical thermal power plant (SACSCTPT) [J]. CLEAN TECHNOLOGIES AND ENVIRONMENTAL POLICY. 2013, 15(1): 133-145.

17 Cui Yinghong, Yang Yongping, Yang Zhiping. Coupling mechanism of solar-assisted coal-fired integrated thermal power generation system [J]. Proceedings of the CSEE, 2008, 28: 99–104.

18 neration system and performance analysis[J]. Science in China Series E: Technological Sciences, SP Science in China Press, 2008, 51(8): 1211–1221.

19 Cui Yinghong, Yang Yongping, Zhang Zhizhi. Solar-coal complementary power generation system and complementary mode [J]. Proceedings of the CSEE, 2008 (05): 102-107.

20 PENG S, HONG H, WANG Y et al. Off-design thermodynamic performances on typical days of a 330MW solar aided coal-fired power plant in China[J]. Applied Energy, 2014, 130: 500–509.

21 PENG S, WANG Z, HONG H et al. Exergy evaluation of a typical 330MW solar-hybrid coal-fired power plant in China[J]. Energy Conversion and Management, 2014, 85: 848–855.

					<i>13.04.01.2020.286.YY EN</i>	<i>page</i>
						73
<i>Изм</i>	<i>Page</i>	<i>Document #</i>	<i>Signat.</i>	<i>Date</i>		

22 Han Tao, Zhao Rui, Zhang Shuai, Yu Xuehai, Liao Haiyan. Research and application of carbon dioxide capture technology in coal-fired power plants [J]. Coal Engineering, 2017, 49 (S1): 24-28.

23 Kanniche M, Gros-Bonnivard R, Jaud P, et al. Pre-combustion, post-combustion and oxy-combustion in thermal power plant for CO<sub>2</sub> capture[J]. Applied Thermal Engineering, 2010, 30(1): 53-62.

24 Plaza M G, García S, Rubiera F, et al. Post-combustion CO<sub>2</sub> capture with a commercial activated carbon: comparison of different regeneration strategies[J]. Chemical Engineering Journal, 2010, 163(1-2): 41-47.

25 Wang Zeping, Zhou Tao, Zhang Jigang et al. A comparative study of carbon dioxide capture technology in power plants [J]. Environmental Science and Technology, 2011, 34 (11): 83-87.

26 Soundararajan, R; Gundersen, T; Coal based power plants using oxy-combustion for CO<sub>2</sub> capture: Pressurized coal combustion to reduce capture penalty[J]. Applied Thermal Engineering, 2013, 61(1): 115-22, 15.

27 Brett P. Spigarelli, S. Komar Kawatra. Opportunities and challenges in carbon dioxide capture[J]. Journal of CO<sub>2</sub> Utilization, 2013, 1.

28 Leung, D. Y. C; Caramanna, G; Maroto-Valer, M. M. An overview of current status of carbon dioxide capture and storage technologies[J]. Renewable & Sustainable Energy Reviews, 2014, 39: 426-43.

29 Aouini, Ismael; Ledoux, Alain; Estel, Lionel; Mary, Soazic; Grimaud, Julien; Valognes, Benoit. Study of carbon dioxide capture from industrial incinerator flue gas on a laboratory scale pilot[J]. Energy Procedia, International Conference on Greenhouse Gas Control Technologies. 2011, 4(1): 729-1736.

30 Xiaochun Li; Qi Li; Bing Bai; Ning Wei; Wei Yuan. The geomechanics of Shenhua carbon dioxide capture and storage (CCS) demonstration project in Ordos Basin, China[J]. Journal of Rock Mechanics and Geotechnical Engineering, 2016, 8(6): 948-66.

31 Zeng Qing. Experimental study on the absorption of carbon dioxide by ammonia method [D]. Tsinghua University, 2011.

					<i>13.04.01.2020.286.YY EN</i>	<i>page</i>
						74
<i>ИЗМ</i>	<i>Page</i>	<i>Document #</i>	<i>Signat.</i>	<i>Date</i>		

32 Zhu Dechen. Research on CO<sub>2</sub> chemical absorption technology of coal-burning flue gas [D]. Zhejiang University, 2011.

33 Mi Jianfeng, Ma Xiaofang. Analysis of China's CCUS technology development trend [J]. Chinese Journal of Electrical Engineering, 2019, 39 (09): 2537-2544.

34 Zhao Rongqin, Ding Minglei, Huang Xianjin. Research on the Policy System of Carbon Capture, Utilization and Storage Technology in China [J]. Land and Resources Science and Technology Management, 2013, 30 (03): 116-122

35 Tian Heyong, Wang Wanfu, Wang Renfang, Yu Xiaodan. Research on CO<sub>2</sub> capture technology [J]. Energy Environmental Protection, 2012, 26 (06): 39-41 + 35.

36 Wibberley L. CO<sub>2</sub> capture using solar thermal energy: U.S. Patent Application 12/374,017. 2007-7-17 [P].

37 Plaza JM, Van Wagener D, Rochelle GT. Modeling CO<sub>2</sub> capture with aqueous monoethanolamine [J]. International Journal of Greenhouse Gas Control, 2010, 4(2): 161-166.

38 Tregambi, Claudio; Montagnaro, Fabio; Salatino, Piero; Solimene, Roberto. A model of integrated calcium looping for CO<sub>2</sub> capture and concentrated solar power[J]. Solar Energy, 2015,120: 208-220.

39 Pyong Sik Pak; Kosugi, T. Characteristics and economics evaluation of CO<sub>2</sub>-capturing power generation systems using solar thermal energy and gasified coal[J]. Transactions of the Institute of Electrical Engineers of Japan, Part B, 2000, 120-B(11): 1496-503.

40 Wang, Fu; Zhao, Jun; Li, Hailong; Deng, Shuai; Yan, Jinyue. Preliminary experimental study of post-combustion carbon capture integrated with solar thermal collectors[J]. Applied Energy, 2017, 185(1):471-1480.

41 Liangxu Liu; Jun Zhao; Shuai Deng; Qingsong An. A technical and economic study on solar-assisted ammonia-based post-combustion CO<sub>2</sub> capture of power plant[J]. Applied Thermal Engineering, 2016, 102:412-22.

42 Haiping Chen; Wenhao Wu; Zhongping Wang; Zhiyun Shi; Jing Wang. Energy Consumption Analysis of Coal-fired Power Plant With CO<sub>2</sub> Capture System Based on Solar Energy[J]. Advanced Materials Research, 2012,3:524-527.

					<i>13.04.01.2020.286.YY EN</i>	<i>page</i>
						75
<i>ИЗМ</i>	<i>Page</i>	<i>Document #</i>	<i>Signat.</i>	<i>Date</i>		



43 Rongrong Zhai; Hongtao Liu; Hao Wu; Hai Yu; Yongping Yang. Analysis of Integration of MEA-Based CO<sub>2</sub> Capture and Solar Energy System for Coal-Based Power Plants Based on Thermo-Economic Structural Theory[J]. Energies, 2018, 11(5): 1284.

44 Xie Miaonova, Leytes. Purification of Process Gas [M]. Translated by the Research Institute of Nanjing Chemical Industry Company. Second Edition. Beijing: Chemical Industry Press. 1982.

45 Mao Songbai, Ye Ning, Zhu Daoping. New technology of low partial pressure CO<sub>2</sub> recovery to capture flue gas CO<sub>2</sub> of coal-fired power plants [J]. Chemical Engineering, 2010 (05): 95-97.

46 Zhang Kefang. Energy analysis and optimization of CO<sub>2</sub> capture system of coal-fired power plant with alcohol amine absorption method [D]. Beijing University of Technology, 2015.

47 Liu Rui, Zhai Xiangbin. Calculation and analysis of carbon emissions from coal-fired power plants in China [J]. Journal of Eco-Environment, 2014, 23 (07): 1164-1169.

48 Wu Wenhao. Research on the integration method of trough solar collector system [D]. North China Electric Power University, 2013.

49 Odeh S D, Morrison G L, Behinia M. Modeling of parabolic trough direct steam generation solar collectors[J]. Solar Energy, 1998, 62(6): 395-406.

50 Han Zhonghe, Bai Yakai, Wang Jixuan. Optimization of solar-coal-fired unit thermal system coupling mode and carbon emission reduction analysis [J]. Journal of China Coal Society, 2015, 40 (S2): 524-531.

51 Fu Wenfeng. Research on the optimization of thermal system structure and parameter configuration of coal-fired power station [D]. North China Electric Power University (Beijing), 2017.

52 Liu Liangxu. Effectiveness analysis and optimization of carbon dioxide capture system after combustion in solar-assisted coal-fired power plant [D]. Tianjin University, 2016.

					<i>13.04.01.2020.286.YY EN</i>	<i>page</i>
						76
<i>ИЗМ</i>	<i>Page</i>	<i>Document #</i>	<i>Signat.</i>	<i>Date</i>		

53 Wang Jixuan. Research on the coupling characteristics of the solar-coal-fired thermal system based on carbon capture [D]. North China Electric Power University, 2014.

54 Liu Lianbo, Gao Shiwang, Xu Shisen. Integration analysis of coal-fired flue gas CO<sub>2</sub> capture system and power plant system [J]. Chinese Journal of Electrical Engineering, 2014, 34 (23): 3843-3848.

55 Zhou Luyao, Xu Gang, Bai Pu, Xu Cheng, Yang Yongping. Thermodynamic analysis of multiple utilization forms of recuperation steam extraction superheat of 1000MW ultra-supercritical unit [J]. Journal of Power Engineering, 2017, 37 (06): 495-500 + 512.

56 Ploumen P, Stienstra G, Kamphuis H. Reduction of CO<sub>2</sub> emissions of coal fired power plants by optimizing steam water cycle[J]. Energy Procedia, 2011, 4: 2074-2081.

57 Gan Zhiyong. Optimization of carbon capture system for 1000MW supercritical coal-fired unit [D]. Tianjin University, 2017.

58 Liu Qiang, Duan Yuanyuan. exergy Analysis of thermal system of supercritical 600MW thermal power unit [J]. Chinese Journal of Electrical Engineering, 2010, (32): 8-12.

59 Lin Heyong. Comparative analysis of industrial boiler thermal efficiency test and exergy efficiency test [J]. Industrial Boiler, 2018 (04): 41-44.

					<i>13.04.01.2020.286.YY EN</i>	<i>page</i>
						77
<i>ИЗМ</i>	<i>Page</i>	<i>Document #</i>	<i>Signat.</i>	<i>Date</i>		